



Calhoun: The NPS Institutional Archive
DSpace Repository

Theses and Dissertations

1. Thesis and Dissertation Collection, all items

2021-06

RENEWABLE ENERGYPOWERED HYDROGEN GENERATION AND STORAGE FROM AMBIENT MOISTURE

Heaton, Charles C., V

Monterey, CA; Naval Postgraduate School

<http://hdl.handle.net/10945/67737>

This publication is a work of the U.S. Government as defined in Title 17, United States Code, Section 101. Copyright protection is not available for this work in the United States.

Downloaded from NPS Archive: Calhoun



Calhoun is the Naval Postgraduate School's public access digital repository for research materials and institutional publications created by the NPS community. Calhoun is named for Professor of Mathematics Guy K. Calhoun, NPS's first appointed -- and published -- scholarly author.

Dudley Knox Library / Naval Postgraduate School
411 Dyer Road / 1 University Circle
Monterey, California USA 93943

<http://www.nps.edu/library>



**NAVAL
POSTGRADUATE
SCHOOL**

MONTEREY, CALIFORNIA

THESIS

**RENEWABLE ENERGY-POWERED HYDROGEN
GENERATION AND STORAGE FROM AMBIENT
MOISTURE**

by

Charles C. Heaton V

June 2021

Thesis Advisor:
Second Reader:

Anthony J. Gannon
Walter Smith

Approved for public release. Distribution is unlimited.

THIS PAGE INTENTIONALLY LEFT BLANK

REPORT DOCUMENTATION PAGE			<i>Form Approved OMB No. 0704-0188</i>	
Public reporting burden for this collection of information is estimated to average 1 hour per response, including the time for reviewing instruction, searching existing data sources, gathering and maintaining the data needed, and completing and reviewing the collection of information. Send comments regarding this burden estimate or any other aspect of this collection of information, including suggestions for reducing this burden, to Washington headquarters Services, Directorate for Information Operations and Reports, 1215 Jefferson Davis Highway, Suite 1204, Arlington, VA 22202-4302, and to the Office of Management and Budget, Paperwork Reduction Project (0704-0188) Washington, DC 20503.				
1. AGENCY USE ONLY (Leave blank)		2. REPORT DATE June 2021	3. REPORT TYPE AND DATES COVERED Master's thesis	
4. TITLE AND SUBTITLE RENEWABLE ENERGY-POWERED HYDROGEN GENERATION AND STORAGE FROM AMBIENT MOISTURE			5. FUNDING NUMBERS	
6. AUTHOR(S) Charles C. Heaton V				
7. PERFORMING ORGANIZATION NAME(S) AND ADDRESS(ES) Naval Postgraduate School Monterey, CA 93943-5000			8. PERFORMING ORGANIZATION REPORT NUMBER	
9. SPONSORING / MONITORING AGENCY NAME(S) AND ADDRESS(ES) N/A			10. SPONSORING / MONITORING AGENCY REPORT NUMBER	
11. SUPPLEMENTARY NOTES The views expressed in this thesis are those of the author and do not reflect the official policy or position of the Department of Defense or the U.S. Government.				
12a. DISTRIBUTION / AVAILABILITY STATEMENT Approved for public release. Distribution is unlimited.			12b. DISTRIBUTION CODE A	
13. ABSTRACT (maximum 200 words) This research combines the proven Electrochemical Hydrogen Production and Storage System with a renewable energy source for safe and reliable utilization in Department of Defense and Navy applications. Photovoltaic cells provide the most robust and cost effective renewable energy combined with minimal complexity and weight compared to other available renewable energy sources. Previous research has proven solar panels are capable of consistently achieving the desired energy output levels for hydrogen generation. The critical component of this research is the design and installation of a coupled control system and graphics display to effectively distribute energy from the solar panels to the different components of the generation system while monitoring system status and regulating production autonomously. Once all components function as desired independently, they are combined and assessed to confirm operational viability and a final configuration to maximize practical utilization is investigated. The final product is the fully autonomous coupled system utilizing the implemented controller as well as a capabilities study and a proof of concept report.				
14. SUBJECT TERMS hydrogen storage, electrochemical hydrogen production, solar energy, autonomous energy production			15. NUMBER OF PAGES 87	
			16. PRICE CODE	
17. SECURITY CLASSIFICATION OF REPORT Unclassified	18. SECURITY CLASSIFICATION OF THIS PAGE Unclassified	19. SECURITY CLASSIFICATION OF ABSTRACT Unclassified	20. LIMITATION OF ABSTRACT UU	

THIS PAGE INTENTIONALLY LEFT BLANK

Approved for public release. Distribution is unlimited.

**RENEWABLE ENERGY-POWERED HYDROGEN GENERATION AND
STORAGE FROM AMBIENT MOISTURE**

Charles C. Heaton V
Ensign, United States Navy
BS, Georgia Institute of Technology, 2020

Submitted in partial fulfillment of the
requirements for the degree of

**MASTER OF SCIENCE IN ENGINEERING SCIENCE
(AEROSPACE ENGINEERING)**

from the

**NAVAL POSTGRADUATE SCHOOL
June 2021**

Approved by: Anthony J. Gannon
Advisor

Walter Smith
Second Reader

Garth V. Hobson
Chair, Department of Mechanical and Aerospace Engineering

THIS PAGE INTENTIONALLY LEFT BLANK

ABSTRACT

This research combines the proven Electrochemical Hydrogen Production and Storage System with a renewable energy source for safe and reliable utilization in Department of Defense and Navy applications. Photovoltaic cells provide the most robust and cost effective renewable energy combined with minimal complexity and weight compared to other available renewable energy sources. Previous research has proven solar panels are capable of consistently achieving the desired energy output levels for hydrogen generation. The critical component of this research is the design and installation of a coupled control system and graphics display to effectively distribute energy from the solar panels to the different components of the generation system while monitoring system status and regulating production autonomously. Once all components function as desired independently, they are combined and assessed to confirm operational viability and a final configuration to maximize practical utilization is investigated. The final product is the fully autonomous coupled system utilizing the implemented controller as well as a capabilities study and a proof of concept report.

THIS PAGE INTENTIONALLY LEFT BLANK

TABLE OF CONTENTS

I.	INTRODUCTION.....	1
A.	MOTIVATION	2
B.	LITERATURE REVIEW	7
C.	OBJECTIVES	9
II.	ORIGINAL DESIGN OVERVIEW	13
A.	HYDROGEN GENERATION COMPONENTS	13
1.	Ambient Moisture Collection.....	14
2.	Water Reservoir Tanks	15
3.	Gas Separation and Routing.....	15
4.	Controller and Current Logic.....	18
B.	COMPRESSION COMPONENTS	20
III.	SYSTEM MODIFICATIONS AND METHODOLOGY	21
A.	MICRO ENERGY GRIDS COMPONENTS AND TESTING	21
B.	PANELVIEW APP DESIGN AND OVERVIEW	26
C.	PWM REMOVAL AND DC SUPPLY CONTROL	31
IV.	DISCUSSION	35
A.	SOLAR VIABILITY AND INTEGRATION.....	35
B.	OFF-GRID CHALLENGES	36
C.	CONTROLLER LOGIC AND OPTIMIZATION	40
V.	CONCLUSION AND RECOMMENDATIONS.....	45
	APPENDIX A. INVERTER SPECIFICATIONS.....	49
	APPENDIX B. PWX1500 SPECIFICATIONS AND TIPS	51
	APPENDIX C. PANELVIEW 800 VARIATION STEPS.....	55
	APPENDIX D. CONNECTED COMPONENTS CODE	59
	LIST OF REFERENCES.....	65
	INITIAL DISTRIBUTION LIST	69

THIS PAGE INTENTIONALLY LEFT BLANK

LIST OF FIGURES

Figure 1.	DOD Energy Usage. Source: [1].	1
Figure 2.	Common Fuel Energy Density Comparison. Source: [5].	3
Figure 3.	Steam Methane Reforming Overview. Source: [8].	4
Figure 4.	Microgrid Research Methodology. Source: [16].	8
Figure 5.	Generation Schematic with Renewable Microgrid	10
Figure 6.	Compression Schematic	11
Figure 7.	Shed Layout at Turbomachinery Lab. Adapted from [18].	13
Figure 8.	Electrolysis of Water. Source: [9].	17
Figure 9.	Micro850 Controller without add on Blocks. Source: [23].	19
Figure 10.	Renogy 100 Ah Battery Design. Source: [25].	22
Figure 11.	VAC Power Inverter Front View. Adapted from [26].	23
Figure 12.	Allen Bradley PanelView 800 Graphics Terminal. Source: [27].	26
Figure 13.	Overall Status Screen for PanelView 800	28
Figure 14.	Microgrid Status Screen for PanelView 800	29
Figure 15.	Water Processing Screen for PanelView 800	30
Figure 16.	Electrolyzer Status Screen for PanelView 800	31
Figure 17.	Electrolyzer Subsystem Screen with Nominal Current Setting	34
Figure 18.	Electrolyzer Subsystem Screen with Maximum Current Setting	34
Figure 19.	PWX1500ML Rear View [25].	38
Figure 20.	Lead Acid Hybrid Gel Discharge Characteristics [25]	42
Figure 21.	Inverter Front View	49
Figure 22.	Inverter Rear View	49
Figure 23.	PWX1500 Pin diagram overview. Source: [28].	52

Figure 24. PWX1500 front view and display. Source: [28].....53
Figure 25. PanelView 800 Graphics Terminal rear view. Source: [27].55

LIST OF TABLES

Table 1.	Generation Power Draw Specifications	39
Table 2.	Generation Microgrid Component Specifications	40
Table 3.	Required configuration for specific external control functionality.....	54
Table 4.	Connected Components Variable Overview.....	59

THIS PAGE INTENTIONALLY LEFT BLANK

LIST OF ACRONYMS AND ABBREVIATIONS

CCW	Connected Components Workbench
CF	Controllability Failure
COTS	Commercial Off the Shelf
DC	Direct Current
DOD	Department of Defense
DOD	Depth of Discharge
EAV	Externally Applied Voltage
ELLSU	Electric Liquid Level Sending Unit
FCEV	Fuel Cell Electric Vehicle
GUI	Graphical User Interface
lpm	Liters per minute
MC	Microcontroller
MEG	Micro Energy Grid
PV	Photovoltaic
PWM	Pulse Width Modulator
R&D	Research and Development
SEG	Smart Energy Grid
SV	Solenoid Valve
VAC	Alternating Current Voltage
VDC	Direct Current Voltage

THIS PAGE INTENTIONALLY LEFT BLANK

ACKNOWLEDGMENTS

I would like to thank my advisor, Dr. Anthony Gannon, and second reader, Dr. Walter Smith, for their support in writing and technical advice. I also want to thank LT Joshua Lewis for his advisement in modifying and supporting his work on the Hydrogen rig. It has been my honor to pursue a degree through the 609 Shoemaker Scholarship curriculum under Chairman Hobson as the first class of ROTC selects for the program. I could not have made it here without the unwavering support of my parents, Chuck and Louise, and sisters, Anna and Bobo.

THIS PAGE INTENTIONALLY LEFT BLANK

I. INTRODUCTION

Based on the congressional energy consumption report from 2019, the Department of Defense (DOD) consumes 16 times more energy than the rest of the federal government [1]. Within the DOD’s enormous block shown in Figure 1, 70% of energy is deemed operationally necessary and based on long standing legislation cannot be federally regulated [1]. However, the remaining 30% is deemed installation energy and is regulated by the U.S. government. According to a 2007 report from Col Lengyel (Ret.) on the DOD’s energy usage moving into the 21st century, the relatively low cost of current energy spending (only 2% of the annual DOD budget) has led to minimal changes in consumption on the operational side due to strategic airlift and other airborne forces’ reliance on JP-4 and JP-5 without a viable alternative [2]. The consumption from air-based transportation has also started to cut into operational readiness as fuel is being rationed to squadrons and units across the DOD, including the critical training commands. To avoid further operational restrictions, the addition of abundant and reliable renewable energy sources to reduce installation fossil fuel consumption is necessary.

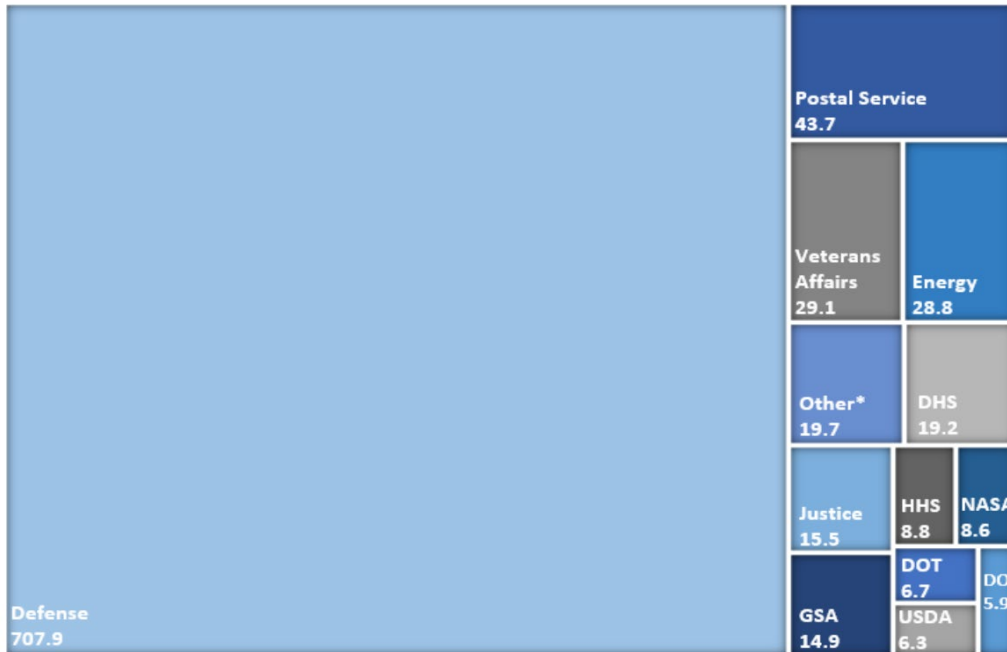


Figure 1. DOD Energy Usage. Source: [1].

Lengyel's [2] report states that since 2003, the DOD has received numerous recommendations for further research and development (R&D) of alternative energy applications for installations including solar, wind, hydrogen fuel cells, and even thermal energy storage. Without a proven renewable energy source capable of providing the versatility and energy density of fossil fuels, the operational energy consumption will never decrease. However, these modern developments of non-petroleum based fuels brings hope increasing sustainable energy supplied across the DOD with possible civilian applications.

A. MOTIVATION

The simplicity of hydrogen, a single proton and electron, along with its incredible abundance has drawn the attention of scientists from many eras. However, the energy potential of hydrogen is often misunderstood; highlighted in Satyapal's 2017 report from the Office of Renewable Energy, hydrogen gas does not hold the same capabilities of hydrocarbon fuels in their combustion efficiency or energy density. Also while Hydrogen is the most naturally abundant element in the universe, it is not readily available in large, extractable quantities like petroleum based fuels [3]. The report goes to state that hydrogen serves as an energy medium capable of high efficiency in advanced fuel cells with energy being released from the oxidation of the element, a reverse process of the electrolysis to be discussed later [3]. Hydrogen's intensive energy density is two sided with its low molecular weight favoring low mass per energy unit but relatively large electron shell hindering volumetric efficiency, thus the need for compression for maximum efficiency.

Once the gas is compressed, it reaches a volumetric energy density per unit volume at least comparable to gasoline and diesel, as shown in Figure 2. There are still benefits of increasing the volumetric energy composition by cooling it to a liquid state however the gains versus the energy required for cryogenic storage are minimal outside of applications with minimal volume restrictions. Using Cummins' recent developments as an example, the high volume required for hydrogen powered machinery is a nonfactor in most non-airborne applications due to lower restrictions or penalties for size [4]. Cummins has developed an effective locomotive with faster resupply times than conventional fuel, only 18 minutes, with 32 hours of endurance for cargo transport. Looking again at Figure 2, the

inefficiency of battery technology is shown in the bottom left corner with less than a tenth of the volumetric energy density of gasoline. The viability and opportunity of natural gas can also be justified in this graphic with 6 to 11% gains in greenhouse gas emissions, lower weight, and less processing required, which plays into the common extraction technique for Hydrogen.

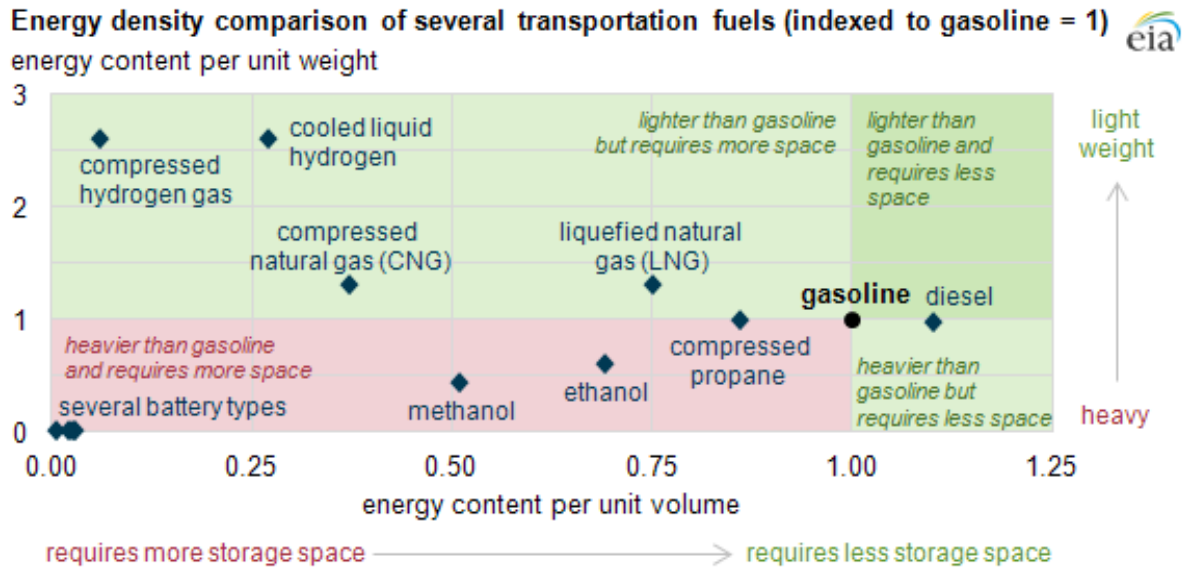


Figure 2. Common Fuel Energy Density Comparison. Source: [5].

Due to low spontaneous combustion conditions, Hydrogen’s safe utilization remains questioned in the public’s eye, similar to nuclear energy, with an ever present fear of a modern Hindenburg accident combined with commercial energy companies not willing to invest in expensive supply chain modifications with only minor increases in sustainability. A transition to hydrogen fuel requires an entire shift in the modern concept of fuel; instead of a supply chain of step by step, large-scale extraction, processing, and transportation installations, hydrogen’s ubiquitous, low-density existence requires small scale “all-in-one” systems providing the fuel at a high efficiency utilizing autonomous operation [6]. Once achieved, these robust, efficient production and storage systems will fill the needs of the DOD in longer range drones than those currently powered by heavy

batteries along with other military instillation applications to reduce the departments carbon footprint by up to 30% [3].

Despite being the most plentiful element in the universe, Hydrogen is rarely found in homogenous quantities due to its ability to bond and including in common compounds like water and ironically carbon-based fuels. Hydrogen is extracted on a large scale using two techniques, steam methane reforming and electrolysis, with the former being responsible for 95% of hydrogen bottled and used in the United States [7]. Steam methane reforming relies on the burning of natural gas combined with water to generate a superheated steam which reorganizes the compounds into two Hydrogens and Carbon Monoxide, which can be combined with more vapor to generate Carbon Dioxide and more Hydrogen, visualized in Figure 3. The efficiency of this reforming has been improved through additions of lead and other membrane catalysts but still relies on the burning of fossil fuels for methane steam generation [8].

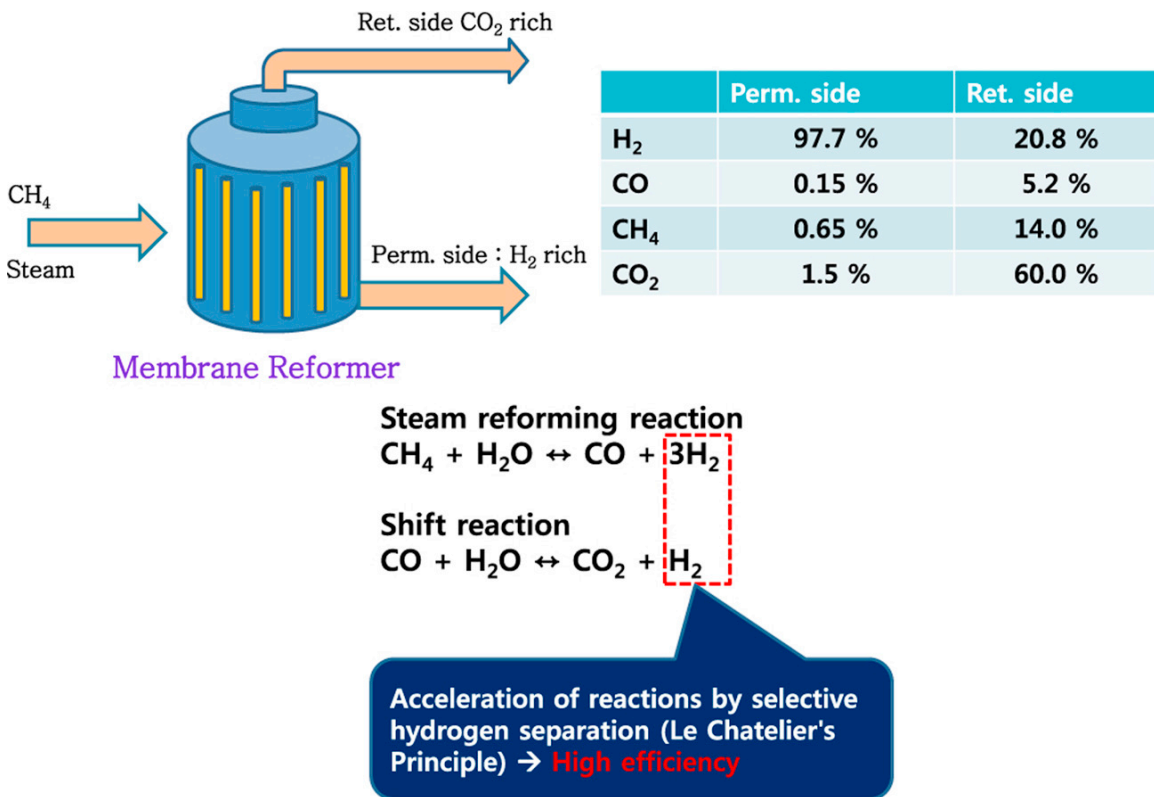


Figure 3. Steam Methane Reforming Overview. Source: [8].

The reason for the favoritism of this method lies in the shift towards natural gas power plants starting the 2000s in the United States as opposed to a full shift to renewable sources such as wind, solar, and nuclear with inefficient energy storage methods. Also, the low cost of natural gas and the required infrastructure give added reason to continue this method of Hydrogen extraction as opposed to single-use, large scale electrolysis. According to the same report from the Office of Energy Efficiency and Renewable Energy, if all vehicles in the United States were converted to Fuel Cell Electric Vehicles (FCEV) utilizing the current Hydrogen production method, the generation of the gas would release as much carbon monoxide/dioxide as half of the original petroleum burning vehicles, a step forward none the less but still a crippling reliance on fossil fuels [9].

Further development of sustainable processes is necessary to enable a future of clean hydrogen and not settling for an imperfect extraction method. This project and other small-scale hydrogen production systems utilize the electrolysis of water, separating the component into its elements. A reason for small scale utilization is mainly for efficiency as well as cost reduction to provide DOD applicable small production with larger scale applications possible. An example of large scale applications are shown in Ulleberg's research report from 2010 [10] highlighting a team from Norway that coupled efficient, medium scale hydrolysis with wind energy and provided the first efficiency metrics for scaled hydrogen production without steam methane reforming. Ulleberg's system was able to power 10 households on a small island for 2–3 days per full system operational day [10]. This test provided 10 years of data to be analyzed by the Norwegian electrolyzer manufacturers and sent the proof-of-concept design to the International Journal of Hydrogen Energy for further development [10].

A renewable energy powered system provides the greatest versatility, minimal environmental impact, and reliability when commercial power is not readily available. Not only does this decoupling with the local grid lead to zero greenhouse gas emissions, the benefits of autonomous hydrogen production and storage provides unparalleled flexibility for the DOD's future Hydrogen fuel cell systems [11]. For an ideal, autonomous "fuel pump" system, The water is sourced from the most common, airborne Hydrogen

compound, ambient moisture, and regulates its own energy utilization to be completely independent of the external environment.

The most significant decision for the system at this scale in favor of robust, unhindered performance is the compression method for maximum energy density. Mechanical compression provides high mass flow and efficiency at larger scales but is not a primary goal of this research as a mechanical system would require routine maintenance and monitoring. To minimize the need for part exchange or oversight at this small scale, a solid-state, electrochemical compressor is incorporated for efficient and effective compression. No moving parts as well as self-regulated power draw contribute to continued compression throughout the night when the stored energy in the battery bank is being utilized. Similar to the electrolyzer, this solid state compressor may be scaled or multiplied to meet the hydrogen compression needs but at a larger scale, mechanical compressors may be required for realistic flow processing as well as meeting the demands of the DOD [12]. This is the likely scenario for final production to generate a viable compressed flow rate of hydrogen gas for drone applications.

To meet the primary goal of autonomous operation, the most critical, required component becomes the controller itself, regulating energy expense for efficient utilization of the available charge as well as simplicity in monitoring the system when required. With a reliance on an expendable energy source, the controller must monitor the charge state of the battery bank and depending on expected energy gain from the panels will trigger different components of the system based on need. For example, if there is a surplus of generated hydrogen with a low charge state, all energy will be applied to the compressor for maximum available compressed Hydrogen. For this proof of concept system, the executable logic is simple enough to ensure safe, low-cost autonomous operation with some user oversight required but increases in size and capabilities would require advanced computing for proper interfacing with the user and account for all possible situations. This is briefly investigated but finding the exact method for system monitoring and logic execution is not primary goal of this work.

B. LITERATURE REVIEW

While the entire system focuses on the generation and compression of hydrogen gas, previous theses from Fosson [13], Aviles [14], and Yu [15] provided sufficient background information about hydrogen as an energy source and design decisions for this rig. As such, a redundant literature review of the viability of hydrogen gas or revisiting of the DOD pursuit of Hydrogen gas alternatives for future mission operability would be trivial. Instead, research was mainly conducted on the options for the microgrid power supply as well as the control system for best implementation of small scale, autonomous system control. This research directly coincides with the primary goals of this thesis of integrating a sufficient renewable energy system while simplifying control for improved ease-of-use.

Implementing a microgrid into this hydrogen system not only adds to the goal of robust operation adding unbounded mobility but also contributes to the sustainability of the system and viability as a clean hydrogen solution as opposed to the current hydrogen generation procedure discussed previously. According to Hossam Gabbar's book on smart energy grid engineering, microgrid solutions lean towards photovoltaic (PV) energy production based on the a minimized carbon footprint, commercial availability, and most importantly the needs of a microgrid [16]. Gabbar continues stating that solar power on average provides the most power regardless of location in the world with at least eight hours of sunlight each day, even with cloud cover. These conclusions were found by utilizing computer simulations based on Solar PV, Fuel Cells, Battery Storage, and the current large scale grid. Figure 4 demonstrates how the simulations were conducted to find the optimal solutions for power requirements from 150 to 1500 kW using micro energy grids (MEG) [16].

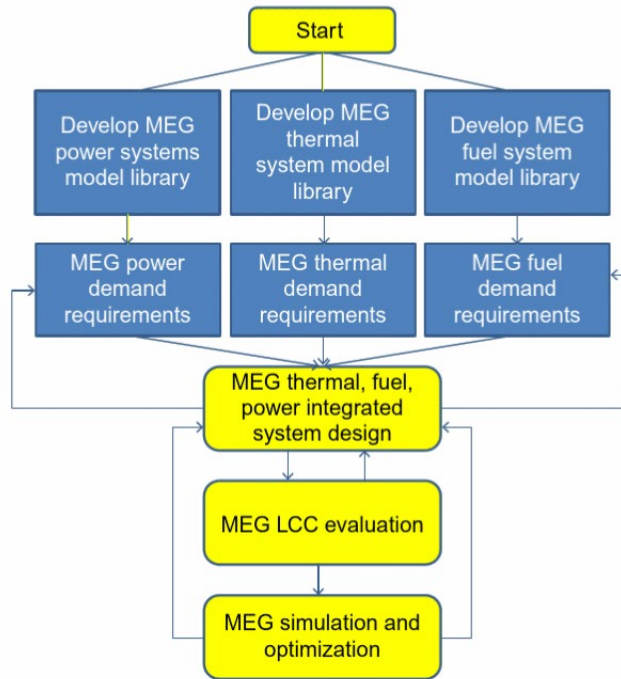


Figure 4. Microgrid Research Methodology. Source: [16].

Due to the fluctuations in energy provided from PV cells and the inefficiency of modern energy storage solutions, smart energy grids (SEG) are designed to utilize fuel cells as a backup for on grid solutions. This contributes to the long term goal of incorporating a supplemental fuel cell into the system to run off the generated hydrogen during times of low power supply (cloud cover or nighttime) and remove the need for a heavy and inefficient battery storage.. This long term goal originated from Aviles' thesis [14] and which also features information about fuel cell efficiency. The most robust system is one that can take whichever energy source is most efficient given the scenario so adding on fuel cells to this microgrid with the current ability to take solar and on-grid input would provide the best proof of concept for system effectiveness and scalability.

Developing a microgrid adds significantly to robust and ecologically minded power generation and usage however the safety factors required for design and operation are often overlooked due to the common reliance on macro grid systems with full monitoring for safety and efficiency. These MEGs must rely on redundant control systems and large safety

factors especially when approaching maximum capacity at a small scale. Some of the major safety concerns addressed by Gabbar [16] include overloading, lack of backup energy, consistent on-site renewable energy utilization, and source selection and integration. Each of these concerns/factors is broken down into impact on users, system, and environment. Due to the simplicity of the rig and low power draw, overload is not likely however the integration of the renewable source and energy storage autonomously without significant redundancy does increase the possibility for harm to system given a controllability failure (CF).

C. OBJECTIVES

In a continuation of the previous work to achieve the goal of autonomous, robust operation, all components will be run off a renewable energy microgrid instead of the current full reliance on commercial electricity. In previous attempts to power this system off renewable energy, only the main generation components, the electrolyzer and dehumidifiers, were powered by the solar panels and the system had no energy storage system. To meet the energy needs of all components and allow for the system to operate during periods of darkness, an efficient inverter and suitably sized battery bank are placed into the microgrid. These new components significantly contribute to the goal of ubiquitous, capable operation and will also add necessary control functions to ensure no part burnout will occur. In alignment with all design methodology from recent upgrades, the components of the microgrid will favor reliability and sustained operation without intervention instead of optimal electrical efficiency. Currently, the entire system, generation, shown in Figure 5, and compression, Figure 6, operates effectively using on-grid power. The goal of this thesis will be to attain production results comparable to on-grid tests with a fully functioning, microgrid-powered generation and compression side and updated controller logic.

The coupling of a sustainable energy source with the many systems involved in generation, compression, and storage requires a further advanced control logic than currently equipped. The controller in use is both cost effectively and sufficiently capable for basic control however the complexity of the system has achieved a level too high for a

basic user to quickly understand the communication intricacies. As such, the secondary goal of this research is to facilitate ease of use of the system by providing a graphic interface between user and system to give insight into how the system is operating autonomously, where any faults may be, and provide user input into the system to override autonomous functionality if necessary. As opposed to pursuing a computer reliant visualization and recording element like past projects set up, a touch screen graphics terminal compatible with the existing controller coding is incorporated and setup for effective and simple monitoring and control.

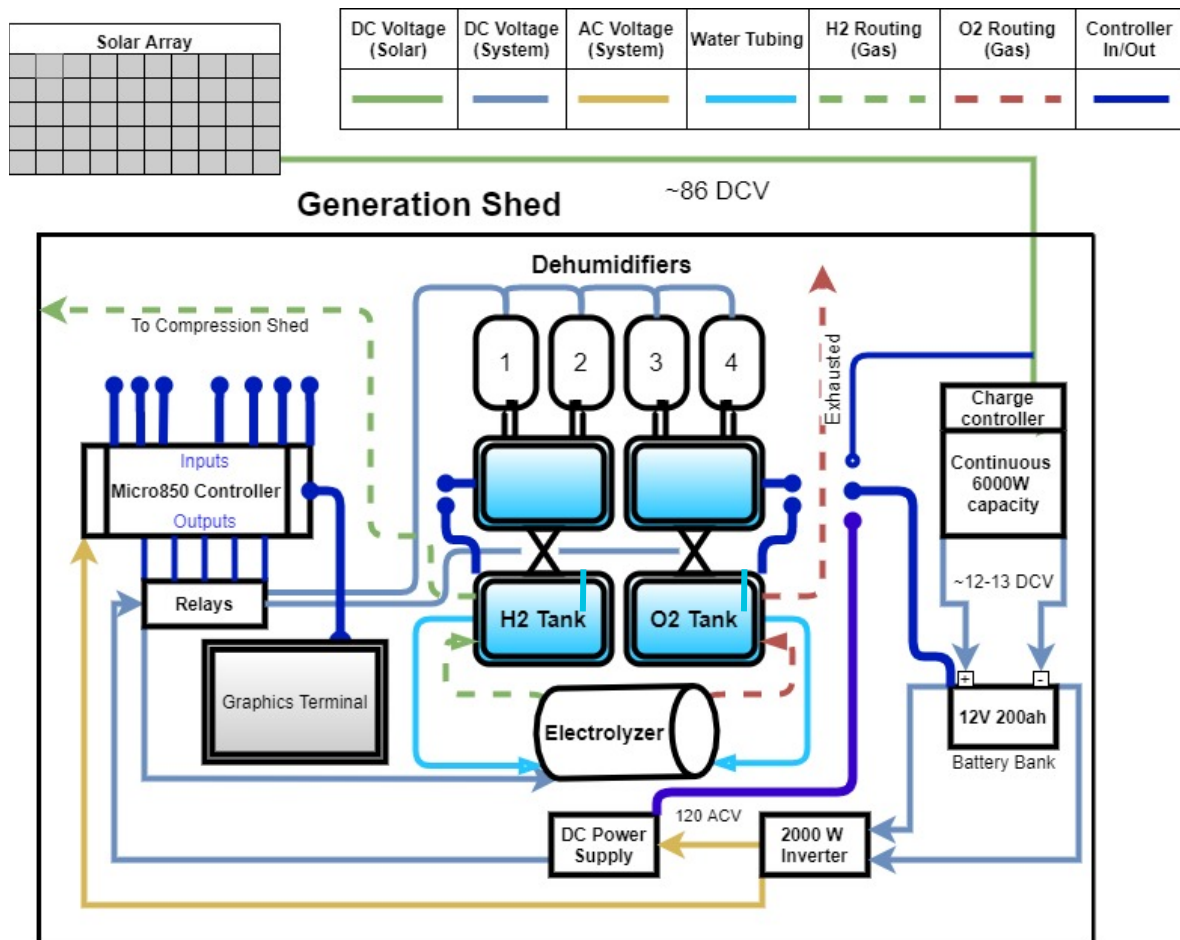







Figure 5. Generation Schematic with Renewable Microgrid

Compression Shed

DC Voltage (.8 VDC)	AC Voltage (System)	H2 Routing (Low Pressure)	H2 Routing (High Pressure)	Controller In/Out
				

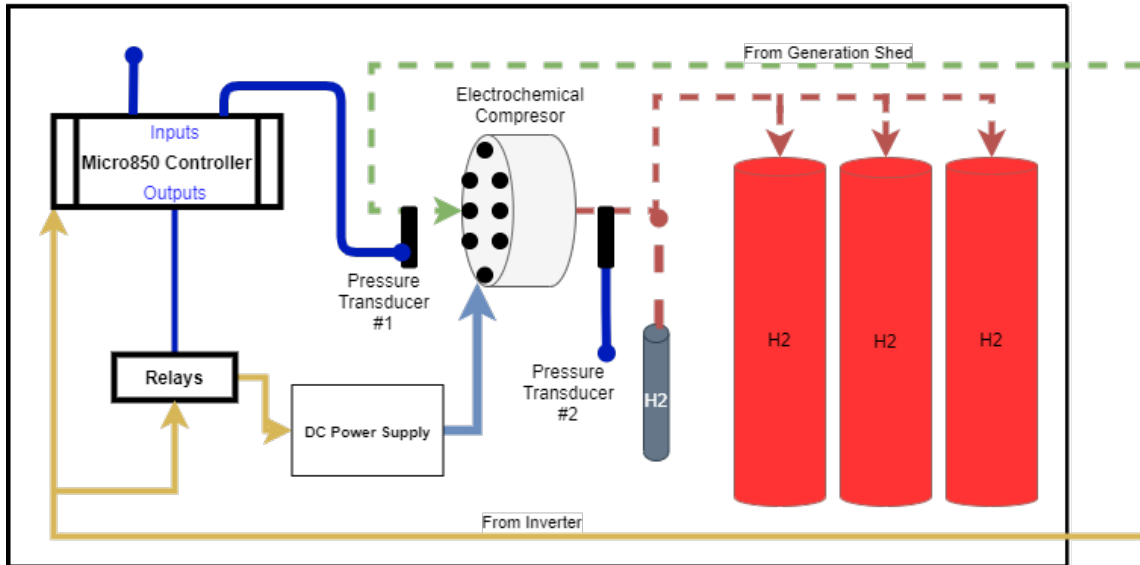


Figure 6. Compression Schematic

The compression systems are also connected to this renewable energy microgrid as shown in Figure 6. The low power draw of the controller and power supply for the compressor lends to independent autonomous operation from the generation side and not need for power management. The startup procedure for the compression system still requires significant user input to ensure high pressure hydrogen safety and maximum hydrogen gas purity with respect to humidity and other gas mixtures. This unfortunately is an unavoidable requirement if the system is not producing and compressing hydrogen for over 3 days.

THIS PAGE INTENTIONALLY LEFT BLANK

II. ORIGINAL DESIGN OVERVIEW

A. HYDROGEN GENERATION COMPONENTS

In keeping with the theme of a proof-of-concept system, the overall hydrogen generation and storage rig at the NPS facility is setup for simple manipulation of or access to components as opposed to the final goal of a minimal volume, mobile autonomous system. The generation and storage components are in separate sheds at the NPS turbomachinery lab. All components are internal, except for the solar panels, to protect against weather and ensure a controlled environment for the dehumidifiers. Also with the current construction at the facility, the solar panels cannot be installed in order to avoid damaging them or receiving skewed results from dust and debris affecting solar efficiency. Furthermore, the location of the entire rig does not favor solar efficiency with the building immediately behind and a series of trees next to the golf course obstructing full sunlight. In the google earth capture in Figure 7 of the location of the rig, the green squares represent the generation and compression sheds on the right and left, respectively, while the red boxes are where the construction is taking place. The section on the roof is where the solar panels used to be located and a deep analysis of the solar efficiency can be found in a previous report from Kevin Hawxhurst [17].



Figure 7. Shed Layout at Turbomachinery Lab. Adapted from [18].

1. Ambient Moisture Collection

The starting point of the generation system is a configuration of four commercial off-the-shelf (COTS) dehumidifiers to provide the system with the necessary pure water, initially installed by Aviles [14]. The dehumidifier units are thermo-electric units produced by Ivation and utilize an electrically induced temperature gradient which reaches the dew point and causes ambient moisture to condense and pool on the surface. They were implemented in Aviles' original design as opposed to other units which utilized compression similar to a refrigerant system or utilized a desiccant material to collect moisture from flowing air [14]. Both systems have critical components requiring maintenance and therefore the thermo-electric unit was chosen due to lack of moving parts and reliability. Aviles' original intention was to generate enough hydrogen for continuous fuel cell operation and energy production and calculated that two units would suffice in producing 1418 grams/day however four were installed for redundancy [14]. Unfortunately, the dehumidifiers severely underproduced the claimed operability as the efficiency of this dehumidifier is directly related to the relative humidity and temperature of the surrounding environment (ideal operation from 5–27°C). Utilizing the electro-thermal gradient, the dehumidifier's heat sinks will over time be incapable of achieving the necessary temperature at or below the dew point to collect ambient moisture. Knowing such, the utilization of these devices in this system is a further extension of the proof of concept more than an attempt at a truly autonomous, robust system. While the dehumidifiers in the coastal Monterey climate have provided enough water for limited tests, ultimately distilled water has been periodically added to the tanks to maintain proper levels for the electrolyzer. As far as electrical draw, these dehumidifiers have had their AC to DC blocks removed and are now all powered directly by 12 VDC from the DC bus. They represent the lowest power draw of the system due to the only resistance component being the thermal blocks; for this reason and the fact that the water supplied is the critical fluid for the entire system operation, the dehumidifiers are configured by the controller to run continuously until the batteries reach levels at which their rechargeability may be affected. As is apparent, this is not the best option for ambient moisture collection and alternative options that meet robust and renewable requirements will be discussed in the suggestions section.

2. Water Reservoir Tanks

Once captured by the dehumidifiers, the pure water is routed directly to the storage tanks via gravity feed tubes. Each storage tank features a KUS Electric Liquid Level Sending Unit (ELLSU) powered by 12 VDC. Each ELLSU has a set resistance based on the position of the bobber in the body of water, in this case the water level of the storage tanks. Each unit has a 240 ohm resistance when the tank is empty and a 33 ohm resistance when full with a travel of 4.2 inches for this particular tank [19]. The ELLSUs provide critical information to the microcontroller, discussed below, as to the available water for the process tanks and will eventually dictate when the dehumidifiers will turn on or off depending on available power.

Each process tank is separated from its respective storage tank by Omega Solenoid valves (SV's) that are actuated by signals emitted by the microcontroller. The SV's take a stepped down voltage from an analog output port on the controller that is engaged based on the controller logic to be discussed later [20]. For safety and to avoid over pressurizing the electrolyzer, the SV's remain closed unless a current is provided. When opened, the reservoir will gravity feed the process tank. Increasing the water level in the process tank not only provides water for the electrolyzer but also maintains the appropriate gas pressure in each respective process tank. The process tanks feature the same ELLSU's as the reservoir and therefore indicate when the tank is running low which is then fed to the controller to act.

3. Gas Separation and Routing

Having now collected the most common and least complex hydrogen-featuring molecule, the water is then split into its respective oxygen and hydrogen components. The benefits of using this electrolysis process are not only sustainable but also scalable in terms of hydrogen production as well as power draw. The charge plates in the system which induce an electron gradient can be added or subtracted as well as grown or shrunk to accommodate the needs of the system. Also in parallel with battery and other energy storage technologies, new research developments are improving the efficiency and lifespan of these plates and other critical electrolyzer components like the semi permeable mesh.

Currently, this rig utilizes a Hydrotube HT5-804 that features 8 plates with a diameter of 4.8 inches [21]. This combination of size and production, rated for 1.7 lpm, are perfect for this proof of concept rig. The lab is also in possession of three other Hydrotube electrolyzers with large and a higher quantity of charge plates; unfortunately these units are not labeled and the company Hydrotube has been dissolved. Therefore, the necessary current provided for these units is not known and out of fear of damage, they are not being used in this new system for better performance [21]. The current HT5-804 unit has been working for 5 years now and it has been found that the main limitation on the flow rate is on the compression side so the utilization of two electrolyzer units in conjunction could increase overall compressed hydrogen production if required. Figure 8 is a diagram illustrating how this electrolyzer functions with the charge plates (gold) and discharges (green and purple) highlighted. From this diagram it is easy to understand how the power supply consistency is critical for sustained operation as a buildup in charge would render the system out of sync with the anode and cathode producing variable amounts of hydrogen and oxygen. Another critical feature for optimal gas production is the water inflow pressure, in this case the level of water in each of the tanks. The control system to regulate the water in the reservoir tanks will be explained in the next section.

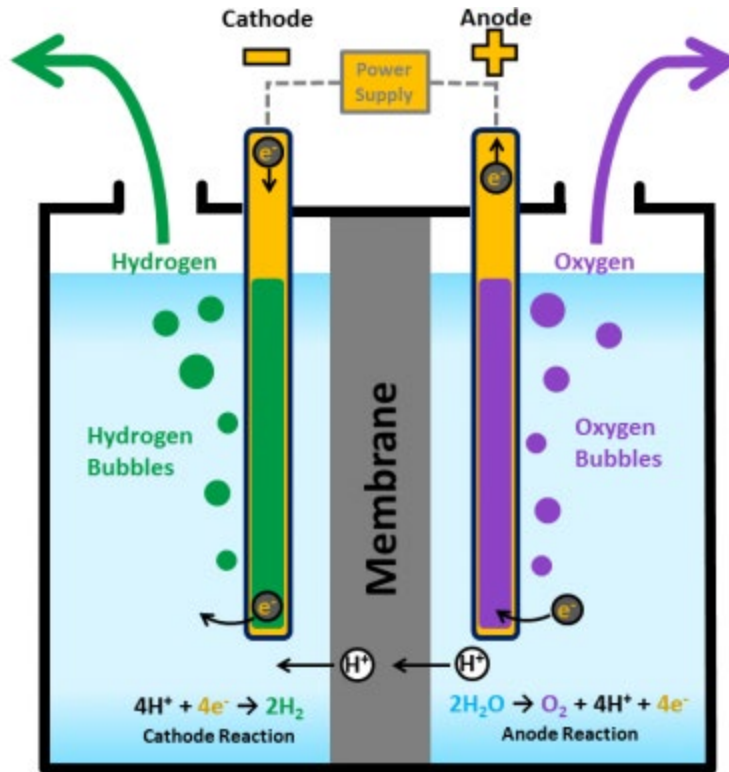


Figure 8. Electrolysis of Water. Source: [9].

The HT5-804 unit takes 12–14 volts and requires a current controller, called a pulse width modulator [21]. Currently, the pulse width modulator connects the 12 VDC bus to the electrolyzer terminals and regulates the current for a relatively constant provided wattage. This PWM is a critical component because it keeps the electrolyzer from overdrawing or overheating during sustained operation. As the electrolyzer is provided charge, the plates heat and this leads to higher current draw based on charge buildup. The role of the PWM is to keep this current draw from increasing too significantly and leading to a blowout of the unit due to overheating of the plates and overproduction of oxygen and hydrogen [21]. Unfortunately this PWM is only able to regulate voltage for the electrolyzer and not other sensitive components, such as the compressor, and cannot be automated due to lack of external, digital input. For this reason, this project will replace the PWM with a DC power supply capable of regulating current for all components on the generation side of the rig.

While this electrolyzer still utilizes a steady state design, the sensitivity of this unit along with lifetime operational efficiency depletion due to water impurity and other external factors ultimately make it the most likely component to need attention and maintenance. Fortunately, a purchase order from November 2020 indicates that the U.S. Navy has signed an exclusive contract with Nel Hydrogen for continued procurement of PEM Electrolyzers [22]. These electrolyzers are currently onboard all Nuclear submarines in order to provide oxygen for the crew with the hydrogen being discarded. The Navy's faith in these electrolyzers to provide on station operability for these submarines is a solid assurance that if large scale production of these rigs is required or an upgraded electrolyzer is needed, the Navy has an existing supply chain [22].

4. Controller and Current Logic

As a first step towards autonomous operation, the compression rig is currently outfitted with a Allen-Bradley Micro850 microcontroller (MC) coupled with multiple analog and digital input/output blocks. This MC runs off of 24V DC power supply, utilizing a transformer block to convert wall AC to a usable current [23]. The Ethernet, USB, and Serial input/output ports allow for easy modulation of the control code stored within and manual control if necessary. Currently this Micro850 is only regulating the generation side of the rig as the cost and complexity of wiring the high-pressure components would hinder the compression side from autonomous operation. The compression side does have its own Micro850 however this has limited functionality as it simply reads data from the pressure transducers and works on a basic logic to close the relay switch to the compressor. A high pressure automated system would put the system into a more restrictive category for hydrogen gas pressurization which would require a significant amount of effort put into safety measures and oversight. Figure 9 shows the layout of the Micro850 without any blocks. It can take up to three normal and three extension blocks [23].

The inputs begin with the provided current to the battery from the charge controller to indicate when the solar panels are providing power and how much. Thesis work from Sun Feng Yu highlights the expected available power supplied by the solar panels throughout the day which is compared to actual data from this transducer [15].

Comparisons not only offer efficiency insights but also may lend value towards increasing the number of panels or configuration.



Figure 9. Micro850 Controller without add on Blocks. Source: [23].

The next input in the system is the voltage provided to the electrolyzer by the DC power supply after running through the PWM. This reading allowed the system to confirm when the electrolyzer is running and therefore using water from the process tanks. For less redundant control, it will be reconfigured to indicate the voltage of the batteries to ensure no battery damage from overdraw. Battery voltage will also dictate which loads will be applied to the batteries during periods of minimal recharge from the solar panels to maximize efficiency and utilization of power for critical components of the system that have low power draw. Another voltage transducer indicates the voltage provided to the dehumidifiers with a similar logics. Because the dehumidifier converter blocks have been removed, the DC voltage provided to the units must be closely regulated to ensure there is no excessive current feeding the system which would damage the functionality of the heat sinks.

The output of the MC are currently all analog voltage switches routed from the analog section of the controller itself or the added output blocks. The outputs serve the purpose of executing the controller logic by triggering a series of arrays for all operating components on the generation side. The arrays are all steady state in keeping with the goal

of high reliability, low maintenance requirements however mechanical arrays may be required for additional safety factors if the system is scaled.

B. COMPRESSION COMPONENTS

As there were not modifications to the compression side in this work and the compressor to be in used in a final design is to be determined, a simple overview will be offered with reference to Lewis's work [24] in finding solutions for some of the flaws in generation capacity and "wet" hydrogen production. The electrolyzer separates the gases effectively however water vapor is the medium for storage in the process tank and therefore the hydrogen gas is contaminated with this vapor as it travels to the compressor. This hydrogen does not meet the criteria for compressed storage even with a specialized drying system however this moisture may be removed during compression. Lewis' work [24] attempted to remove the moisture with a series of drying apparatuses prior to the compressor but these devices were not successful and a recommendation of a new compressor was made. For this reason, the compression side of this rig may need to be modified for a full proof of concept capable of generating clean hydrogen and significant steps were not made to improve autonomous operation.

III. SYSTEM MODIFICATIONS AND METHODOLOGY

In keeping with the primary goals of renewable energy reintegration and facilitating ease of use, robust, new components for energy processing and storage are incorporated and interaction with the Hydrogen generation system has been simplified to a single graphics terminal and custom app. The project shifted towards the ease-of-use goal for monitoring along with implementation of more advanced systems such as the PWX power supply and an Allen Bradley graphics terminal. The hardware on hand was investigated for potential application to this project and others around the lab. Ultimately, the findings of this investigation led to substantial simplification of autonomous system design as well as proper utilization of modern technology. These subsections will discuss the final microgrid configuration with operational status and test results, the graphics design and functionality, and the removal of the PWM and replacement with the PWX.

A. MICRO ENERGY GRIDS COMPONENTS AND TESTING

Starting with the primary goal of this thesis, each of the new energy processing components between the solar panels and the hydrogen manufacturing subsystems will be highlighted to give an overview of the improved renewable energy micro-grid. The modifications made to the control logic have been discussed but the redundant protections within these new components add to safe operation of the system and contribute to the goal of a fully functioning renewable energy microgrid that functions autonomously based on single input from the Micro850.

Directly connected to the solar panel distribution box is the charge controller. This charge controller was the only component between the panels and hydrogen generation components in past iterations utilizing renewable energy. The additional components are meant to take stress off the controller and implement better control for efficient utilization of an expendable power supply and increase ease of use with self-regulating equipment. The in depth specifications of the charge controller in use may be found in Sen Feng Yu's thesis [15] and will not be discussed further here due to the lack of solar panel installation during research.

The charge controller then directly wires into two Renogy 100 Ah, 12 VDC batteries. These are lead-acid gel hybrid batteries with desirable deep discharge characteristics and are cost advantageous in comparison to lithium ion batteries [25]. The battery amperage sizing was based off of power expense when running the dehumidifiers alone along with the controllers in the generation and compression sheds. Preliminary tests put the energy usage of the controllers and valves without any relays closed at 4.6 amps while each of the dehumidifiers utilizes approximately 2.7 amps. Ideally, the system would be capable of producing water and maintaining autonomous operation during the nighttime or during inclement weather, approximately 12 hours averaged over the entire year. With this in mind, the necessary size for 12 hour operation of 15 amps worth of equipment with a 90% DOD to avoid overdraw is approximately 200 Ah. The weight of a single, 200 Ah lead-acid battery is over 120 pounds so two 100 Ah batteries in parallel were chosen. The controller logic was written to avoid dropping below 50% DOD for longevity and shuts off the dehumidifiers at this point, lowering the energy usage to only 4.6 amps. Figure 10 shows an expanded animation of the build of the Renogy gel deep cycle battery.

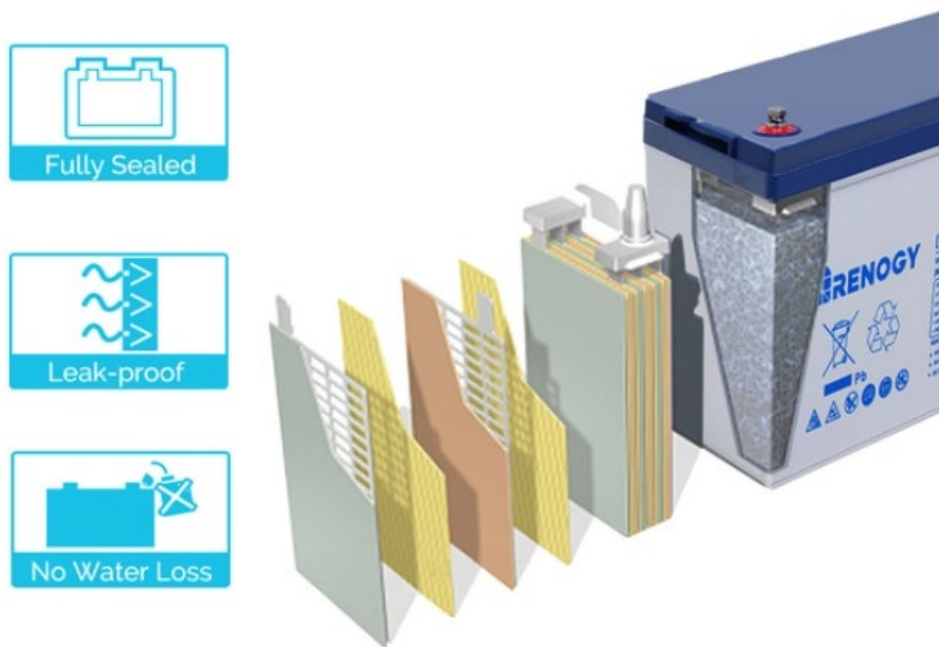


Figure 10. Renogy 100 Ah Battery Design. Source: [25].

From the battery stems the first energy processing component in the inverter. The model equipped is an AIMS Power 12 VDC to 120 VAC pure sine inverter with a 2000 W nominal capacity [26]. The reason for immediately taking the VDC from the batteries and charge controller and converting to VAC is to power the smaller components in the system as well to have fully renewable system. After testing with the power supplies, this inverter is 92% efficient in voltage conversion and importantly features a VAC bypass option with automatic switchover [26]. This means that the entire system may be pulled off of the renewable energy source and routed back to grid power automatically when required. Such a scenario might be if maintenance is required for the solar panels or if the batteries need a long duration charge to bring them back to peak efficiency. Figure 11 shows the front face of the inverter with the power switch and LED indicator in the lower left and VAC routing on the right. The VAC input is currently an adapted extension cord while the output is a power strip with three permanent plug-ins: a separate power strip for the generation controller and monitoring devices, the PID and water transfer valves, and an extension cord to the compression shed to power all compression components. The other available plugs on the strip are open for the PWX1500 which cannot be kept in the shed for long period due to environmental concerns. The VDC inputs are on the rear of the inverter and are connected via 4 AWG wire. More information about the inverter operation can be found in Appendix A.



Figure 11. VAC Power Inverter Front View. Adapted from [26].

The final component of the MEG is the PWX1500ML DC power supply and holds the key controllability component behind the design of these energy processing components. Running off the VAC provided by the inverter, the power supply receives and transmits voltage and current settings to and from the Micro850 controller via proportional voltages. Information about the specific voltage readings transmitted to and from the device for read/write capability can be found in Appendix B. This Appendix also features instructions for configuring the power supply to take control inputs from the controller as well as general information about functionality. As was discussed in the PWM removal section, the constant current control of the PWX1500 is the entire reason for developing this smart micro-grid. Instead of relying on basic relays and modulation blocks, the losses from converting power from the batteries are minimal when the gains are complete control of the system along with redundant alarm and monitoring features. If communication is lost with the controller, the power supply will automatically cut voltage applied instead of continuing to power the electrolyzer while the code itself will also open the relay to the DC components to stop power applied. In the case of overdraw to the system (i.e., the batteries are low and not being charged), the code will open the relays and if they are not opened, the power supply will reduce output and produce audio and visual alarms indicating low voltage. There may be a case where the power supply alarms are triggered while the batteries are still sufficiently charged due to losses from the inverter, but this scenario would lead to the inverter sounding audio and showing visual alarms of low voltage applied when it drops below 9.8 V. This triple redundant system means that a user needs to know little about the system to operate and assuming all components are working properly, the Micro850 can regulate all system functions in one place while displaying all critical information.

Once all MEG components were wired in, basic functionality tests were conducted to show the minimal losses as well as improved controllability and observability of the system. During normal operation with the mimicked solar and battery supply, the system drew 41.2 A at 12.25 V. The charge controller is capable of meeting this demand during normal conditions in Monterey. To mimic the discharge of the batteries, the voltage of the solar and battery input was reduced to 10.5 volts, at which point the controller shut down

the electrolyzer and reduced power consumption to 29.8 A. The differential here between the expected power draw of the system only operating the dehumidifiers and control systems and the experimental draw is due to the unexpected draw of the massive PWX1500. Even when operating without any output current draw, the PWX1500 needs 8.9 A which becomes approximately 10 A due to inverter processing. These losses were expected in the system with additional components and are necessary for the increased controllability and autonomous operation. A properly sized, smart power supply could be acquired that is better suited for this application with a much lower steady power demand.

Upon dropping the input VDC to 10 V, the dehumidifier relays opened and the alarm sounded on the inverter for undervoltage input. The criteria for undervoltage alarm is $9.8 \pm .3$ VDC and will sound an audible, constant whine. The automatic shutoff is at $9.5 \pm .3$ VDC. The power draw with the dehumidifiers off was 10.3 A which could be broken down to 1.5 A per controller, 1.4 for PID and steady state valves, and 6.4 for the inverter and PWX1500. This would discharge the batteries completely in 20 hours which is the reasoning for monitoring of the system every 48 hours at a minimum to ensure that there are no audible alarms and the system is operating properly.

At this point, the system has become fully autonomous based on the controller logic in the generation and compression shed which feed off each other without the need for wired logic. The only inputs after preliminary setup are the pushbutton on the graphics terminal and the current setting for the electrolyzer. The complexity of a cold startup has been significantly reduced with the only requirements being the installation of the PWX1500 and plug-in of control terminal, ensuring the inverter is in the proper mode, and battery charge confirmation before pressing the master switch to start. The sudden power draw from the PWX1500 may cause the dehumidifiers to switch on and off for a period of 20 seconds at the start, but once at equilibrium, the generation is completely self-regulating while the compression side requires expensive control modifications to routing the high pressure gas through the storage tanks. This, however, is not a priority at the moment based on flow rate characteristics of the current compressor.

B. PANELVIEW APP DESIGN AND OVERVIEW

The PanelView 800 graphics display offers new interaction with all generation components as well as maximum utilization of the advanced Allen Bradley control system. This is the smallest graphics display offered with a touch screen at 4 inches diagonal. As can be seen in Figure 12, it features four push button function keys at the bottom for direct interaction with such a small screen. For this application, the ethernet port was utilized to transmit information from the controller to the terminal and vice versa. Designing the app for the display can be done using the existing connected components workbench software however the drives for the display and controller had to be updated twice in order to ensure the communication script would run properly. Other than efficiency and operability, this system offers added safety for the system with customizable alarms and shutdown logic as well as log function which are able to store data or even transmit any signals or alarms over email or print to a printer.

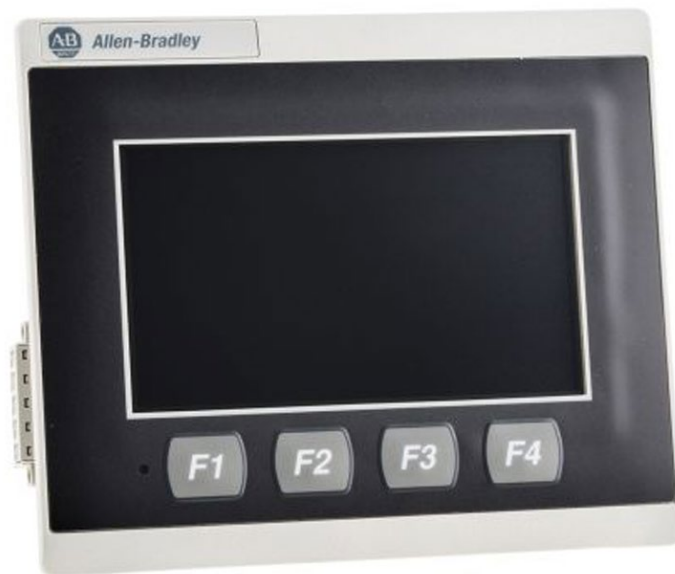


Figure 12. Allen Bradley PanelView 800 Graphics Terminal. Source: [27].

For simplicity, there were four screens developed for generation oversight and control to correspond with the four function keys. The four screens each focus on a different

subsystem for hydrogen generation: Overall Status, Water Processing, Microgrid Status, and Electrolyzer Status.

The Overall status page allows for navigation to each of the subsystems while giving simple information about which systems are running as well as the master on/off switch. The Solar indicator takes the current flowing from the charge controller and indicates whether the panels are providing the battery with charge. The battery indicator will show “DEAD” in red when the battery moves below the minimum effective voltage (10.5V) when the controller logic will shut down all power draws. This will also indicate to the user if the battery is dead and not charging that damage may occur to the battery if the draw from the controller continues and the backup inverter supply is not connected. The Dehumidifier and Electrolyzer indicators show whether the relays for each device is switched on or off. These are useful in knowing which systems should be operating and especially if a user has remote access to the panels, this is better than the basic audio/visual indicators when the systems are on. The large Button on the right is the master switch and turns the autonomous logic on or off. This is a redundant safety system with the emergency stop switch and allows for basic user interface. The time and date log at the top is important for alarm and data logging while the buttons at the bottom correspond to the function keys and allow navigation to over specific pages. Figure 13 shows the status screen under normal, sunny operation.

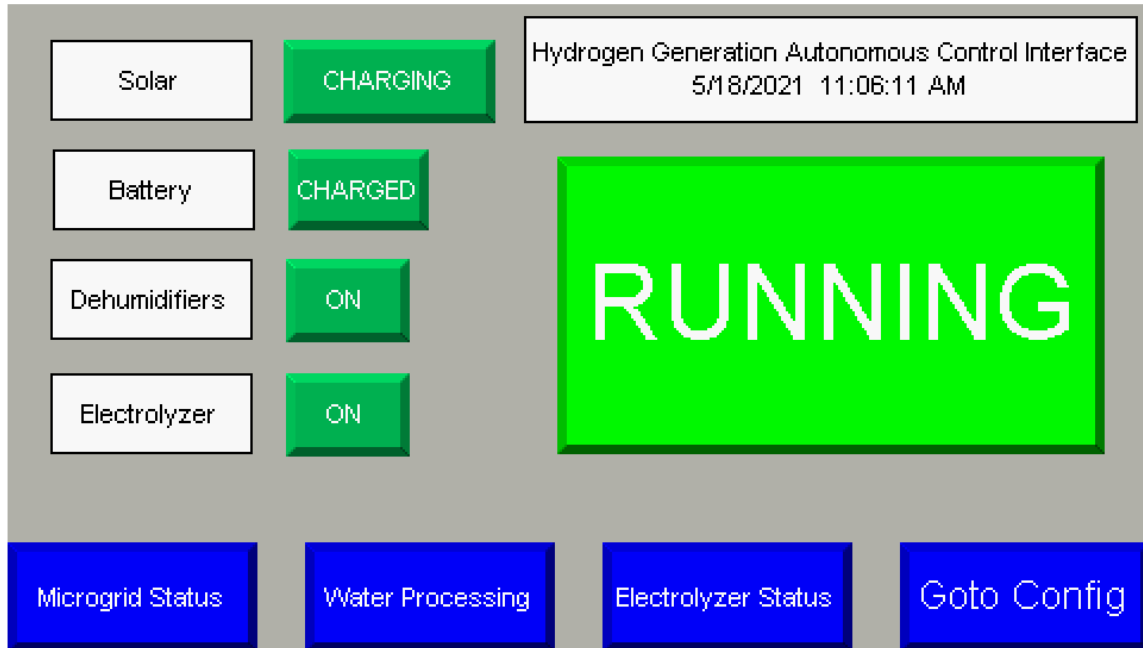


Figure 13. Overall Status Screen for PanelView 800

The second screen is the Microgrid status screen which gives an overview of the renewable energy supply to the system. This screen features a large plot of the battery voltage over a 30 minute interval. This is due to data plotting restrictions and a longer battery voltage plot would be desired for long term monitoring of the autonomous system. Under the charging status is the display for the incoming current from the current transducer attached to the charge controller cable. The battery bank indicator also features a voltage reading directly from the paralleled batteries as well as the current being supplied to the inverter. If increased data point storage was possible, the graph would also show the current supplied over a day to log the available power for autonomous operation decision making. The Home button allows for navigation back to the main screen. The size of the graphics terminal forced the design to have to route back through the main screen to get to different pages. Figure 14 shows the screen under cloudy conditions with a dead battery; the plot could not be shown due to image quality.

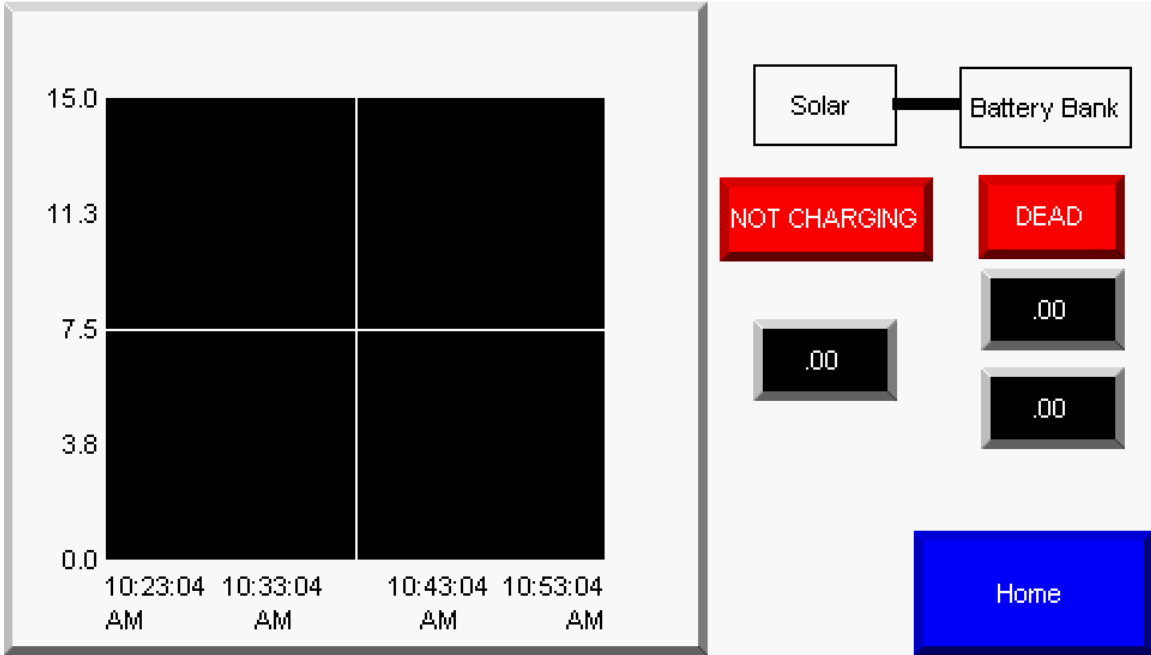


Figure 14. Microgrid Status Screen for PanelView 800

The third screen in order to generation routing is the most in depth and highlights the water processing components. This is where the majority of the controller logic is executed and therefore the most inputs are available. Based on recommendations from Allen Bradley for water pump control, the tanks are situated exactly as they are in the shed with the storage tanks on top with the process tanks below and a pneumatic valve in between. The valve status is displayed in the bottom left to ensure the user that the valves are closed and the process tanks are not being excessively filled. The tank levels are indicated both numerically and visually; the numbers displayed beside each tank correlate to the water height in each tank in inches. The bar indicator inside of each tank image displays the height of the water relative to the tank size. As the source of all of the water used in the system, the dehumidifier status indicator is in the center of the page to show that water is being made from the ambient moisture. Figure 15 shows the Water Processing screen, again unfortunately without active indication due to image quality.

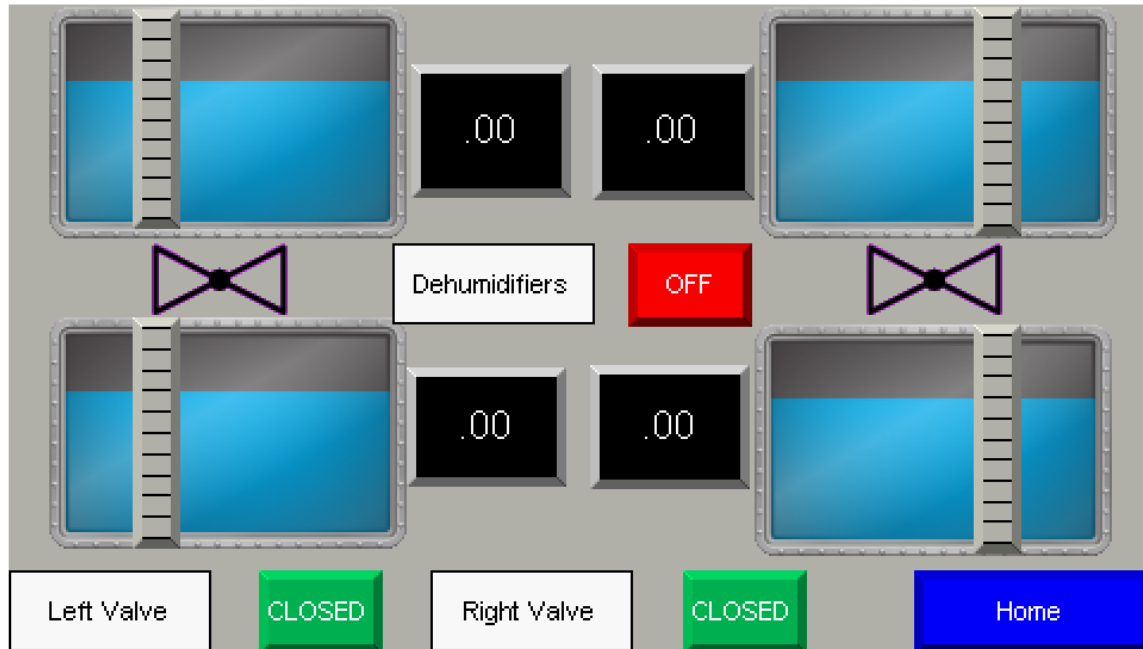


Figure 15. Water Processing Screen for PanelView 800

The final specific monitoring screen is the most significant as it shows the entire status of the electrolyzer. This screen could be improved with advanced inputs (flow rate, temperature, etc.) as discussed previously but at the moment the most critical monitoring components are the voltage and current applied and process tank levels. The visual indicator of the electrolyzer allows for adding of these components in the future but currently is mostly just a place holder with an estimated flow rate of hydrogen displayed. The output voltage and current are directly provided by the DC power supply and with the removal of the PWM, proper voltage application is critical to avoid damage. That is why this screen allows the user to set the production state as nominal or max output with the button at the bottom. Max output set the DC power supply to allow up to 4 amps extra applied current and a voltage jump of .5V. The graph here monitors the tank levels of the process tank as these are critical in understanding if there is a problem with the production, the oxygen exhaust, and/or the storage tank feed system. If the graph shows a single line, the system is operating normally. Figure 16 shows the electrolyzer status under nominal operation.

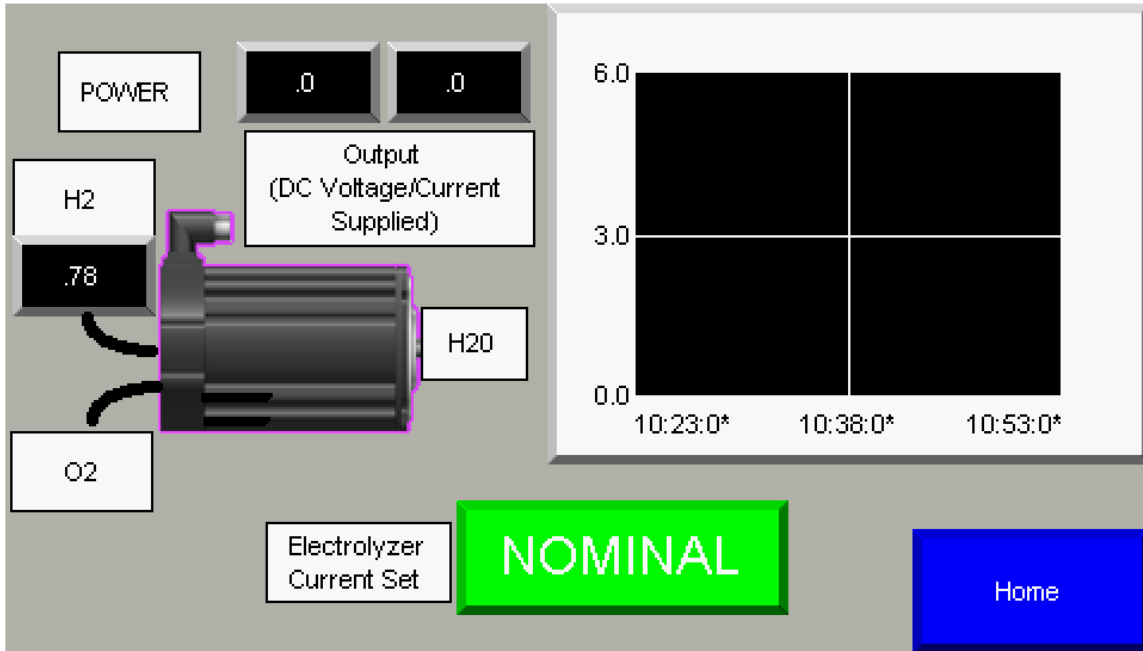


Figure 16. Electrolyzer Status Screen for PanelView 800

The graphics provide insight into the operation of the system for almost any user, regardless of operational experience or understanding by using visual cues of the actual setup of the components such as the water tanks and electrolyzer. This is yet another critical step towards robust operation as the universal hydrogen fuel pump is a small, autonomous system where this display may tell users when the hydrogen will be ready for use and if everything is operating properly. Steps taken to update or troubleshoot this graphics terminal may be found in Appendix C.

C. PWM REMOVAL AND DC SUPPLY CONTROL

The removal of the PWM contributed to both motivation points in that it increased the reliability and proper utilization of the renewable microgrid along with increasing the ease of use of the system. The PWM's manual input dial required decentralized input from the user and an increased understanding of the system. If it remained in the system between the DC power supply and the electrolyzer, it would not only be a useless redundancy that failed to contribute to robust operation but also hinder control efforts to regulate hydrogen

production automatically. With this reasoning in mind, the following chapters explain the simple methodology and added controllability and reliability after removal.

Due to the uniqueness of this specific electrolyzer, steps were taken to ensure removing the PWM would not lead to any other unforeseeable failures. The manual for the Hydrotube Electrolyzer clearly states that the PWM must be installed but this is bypassed based on two factors. This first factor is this manual assumes that the hydrotube is being powered by an unregulated energy supply with no restrictions on current flow to the electrolyzer. This is not the case for this new system as the PWX1500 features constant current and constant voltage control. The second factor is that Hydrotube inc. was the only seller of these PWM units and their website states multiple times that there are no other reliable PWM units on the market, leading to the assumption they were attempting to monopolize. This is the logic used in removing the PWM while still maintaining safe operation of the electrolyzer.

To confirm the PWM would hinder the controllability of the system by the PWX1500, tests were conducted with the PWM still in operation being fed by the DC power supply. The PWX1500 features advanced constant voltage control, superior to that of the PWM as was showcased in varying the voltage applied from the power supply versus the PWM. The power supply was set to output a constant 12.5 VDC and no more than 12 Amps to the electrolyzer. The PWM was then manually set to allow 12 VDC through using the manual knob however the variability of the applied VDC was almost 30 mV. Now switching to constant PWM input with varying power supply application, the PWM constricted the applied VDC to 12 V as designed despite varying the power supply up to 15 V and allowable current up to 17 amps. This is an example of how the PWM would render any proportional control changes to the power supply useless as whatever the setting is on the PWM will ultimately dictate the applied charge. These tests were successful and the PWM terminals were removed from the system and replaced with 10 AWG wire directly from the switch box to the system.

To ensure that the PWX1500 was capable of properly regulating applied charge to avoid overvoltage, a full scale test with a mimicked solar input and battery supply was conducted. A mimicked solar and battery system was required as the batteries had still yet

to arrive nearing the thesis deadlines and the panels could not be setup on the roof due to construction still being carried out. This mimicked battery bank consisted of a separate PWX1500 applying a constant 12.5 VDC to the inverter as the batteries would in the parallel configuration. The full configuration is discussed in the next section. The permanent PWX1500 in the system was hooked up to the controller via proportional control and monitoring terminals and then connected to the circuit box to supply charge to the electrolyzer and dehumidifiers. The autonomous system was turned on and monitored for any alarms. An overvoltage alarm has been set for the electrolyzer if the voltage transducer exceeds 13.1 volts however this is impossible as the voltage applied is directly controlled and monitored by the Micro850 and has an output upper limit of 1.625 V, corresponding to proportional control of 13 V. The current control regulation was tested from the graphics controller and resulted in proper charge control to the electrolyzer and tangible flow rate change, as designed. This proved that the PWX1500 in conjunction with the new MEG is capable of regulating charge to the electrolyzer via the Micro850 controller, autonomous controller logic, and user input for flow rate control. Figures 17 and 18 show the electrolyzer subsystem screen when the current setting is changed. The change in current and voltage applied can be clearly seen in the top left corner and was constant for each setting throughout testing based on the cycling of the electrolyzer.

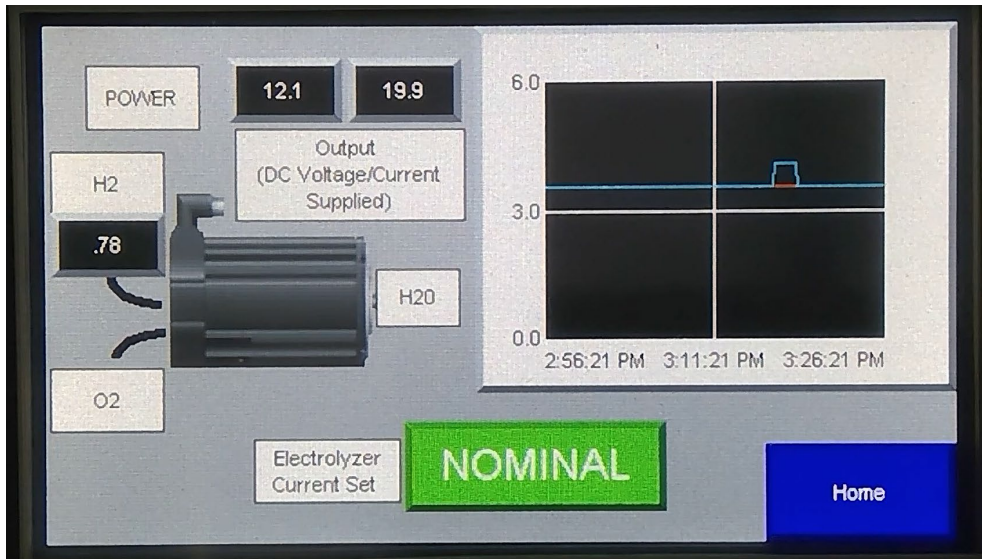


Figure 17. Electrolyzer Subsystem Screen with Nominal Current Setting

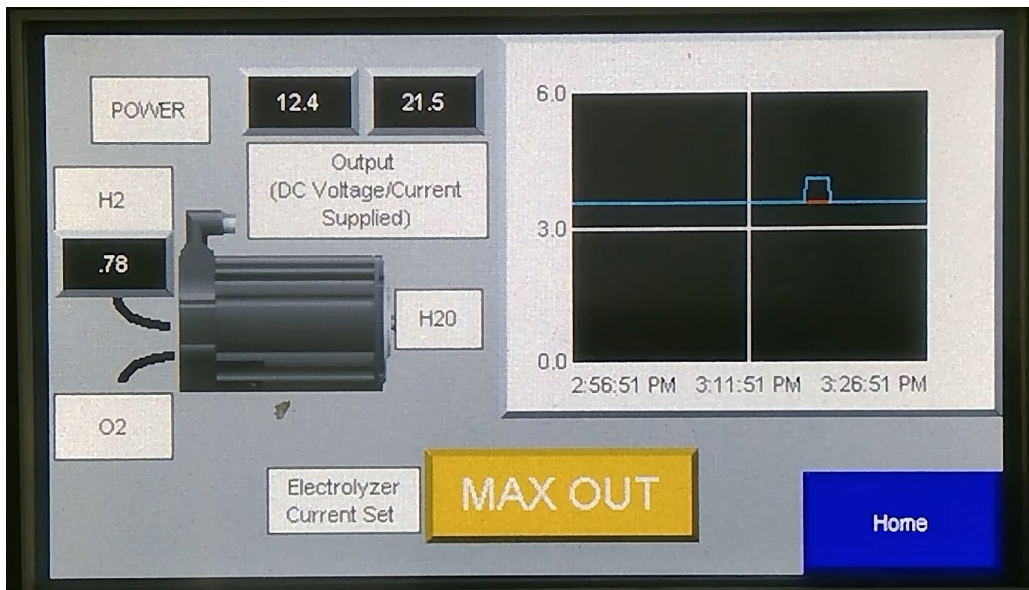


Figure 18. Electrolyzer Subsystem Screen with Maximum Current Setting

IV. DISCUSSION

The modifications made to the generation rig were almost entirely focused on the controller logic and interaction with each system as well as the power sourcing itself. There was limited modification of the wiring into and out of the controller or with the routing of water and hydrogen through the system. The controller inputs provided enough information for a sufficient autonomous operation controller logic similar to that already in place. The labeling of systems provided by Lewis [24] also significantly simplified the data flow.

Incorporating new hardware into the system for renewability was the main focus of the project originally but delays in funding for the project shifted the focus to understanding the controller software, Connected Components Workbench (CCW), as well as the DC power supply, Kikisui PWX1500ML, and its supplemental code and voltage regulation software. This digression led to the pursuit of a graphics interface for the generation system and added another robust and simplified component to the system, another step towards the ultimate goal.

A. SOLAR VIABILITY AND INTEGRATION

Solar panels were once integrated into this system in order to attempt a renewably powered system however the limited components available for a true microgrid were not originally available. The solar energy was fed to the charger and then directly into the system without necessary control and regulation. This led to burnout of the charge controllers due to varying power draw and ended with the return to reliance on wired power. Yu [15] found that solar power could provide the necessary energy for the system however without the necessary components in between, there was no way to harness the energy effectively. Also the wattage rating for the charge controller is right at the capability of the nine solar panel configuration, another reason for charger burnout in previous attempts.

With new components available for a true MEG, the solar panels are able to be fully harnessed with peak time power collection almost at 100% capacity if necessary for the system. Unfortunately, due to construction and maintenance on the building adjacent to the

sheds, as highlighted previously, the solar panels have been inoperable for the majority of the past 12 months. This coupled with the lack of hardware made it difficult to conduct further tests on the energy capacity of the new system.

To mimic the solar array and ensure maximum capacity of the batteries during tests, the PWX1500 as well as a basic battery charger were equipped. While these systems bypassed the charge controller meant for the solar panels, the data from Yu's report is sufficient to show that the controller functions properly in this solar configuration. The battery charger was used for basic discharge tests to see how the system drew from the batteries under base conditions in order to write the proper controller logic for optimal power utilization. The PWX1500 was used to mimic the incoming charge from the charge controller as if the solar panels were providing energy to the system. Unfortunately, the second PWX1500 required for these tests was taken for use by another project on site so these tests were limited and a reliance on the battery charger was necessary but still provided adequate tests runs for the system under "renewable" power.

The MEG itself will be fully wired in the final diagram for this thesis however the lack of solar panels during the research period made it impossible to test this configuration fully. As such, a proof of concept will come from each component working properly independently and the combination of this data will suffice in moving towards the next steps of autonomous operation and compression powering.

B. OFF-GRID CHALLENGES

There are two main problems that introduce themselves when developing a renewable energy MEG. The first is accounting for lack of provided power by the renewable source and ensuring the system adequately utilizes available power without breaking any components due to low voltage or depleting any storage capabilities. This can only be achieved through proper logical control and implemented by an MC. Especially for a fully autonomous system with self-regulation, the control logic must include all components as there is not an operator to manually engage or disengage individual systems on the generation side. Most MEGs function autonomously with the intent of meeting power demand independently however this system is fully coupled and the microgrid must

be able to function with individual system parts. The Micro850 can properly execute and distribute logical control on varying scales due to the expansion packs and attachments however there are even limitations there based on simple logical and specific voltage outputs which may not couple properly with all the COTS components.

An example of this difficulty in physically implementing the logical control is in regulating the PWX1500ML power supply that is wired into the system. According to the instruction manual, the PWX has the ability to regulate current and voltage output based on an externally applied voltage (EAV). The supply can take the EAV and vary the DC output voltage and current based on a specific range. The low range setting divides the EAV by 5 and multiplies this by the set voltage and current. The high range setting does the same but now divides the voltage by 10. The difference in these settings is the power supply has a tight threshold for variability of the EAV so if more values of output voltage or current are required then there must be a higher range of values. Also due to such a threshold, the inputs for each of the settings is limited to EAVs between 0 and 5 V and 0 and 10 V respectively. Anything above 10.5 V will cause irreparable damage to the internal components of the supply. External control of this DC power supply would allow for variance of the current provided to the electrolyzer; this would be required for a fully autonomous system as the mass flow provided to the compressor must not exceed working tolerance and must be slowed to avoid excessive forward pressure on the membrane. This was the entire reason for integration of such a sophisticated DC power supply however unfortunately here lies the difficulty in executing the logic. The Micro850 OB16 block is capable of digital outputs to powering small components beyond a simply relay switch. The operating voltage range of this block and similar Allen Bradley components is 10V to 50 V. The extra hardware that would be required to step down these DC voltages in order to make the signal suitable for the power supply would lead to further unreliability and signal tolerance loss meaning there could be an accidently oversupply of current to the electrolyzer which leads to a failure.

To get around this control limitation, the input/output configuration of the generation system was revised to accommodate the dc power supply variations. Due to the connection between the two water storage tanks, reading the water height of each tank is

redundant and unnecessary. Therefore, the voltage output being used to read the tank level height may be reconfigured to now provide EAV to the power supply to vary the applied current. There are also open terminals in the IF4 block on the controller in order to receive voltage signals from the PWX correlating to the output voltage and current. This allows for accurate readings and regulation of the current and voltage applied to the electrolyzer due to constant current draw from the dehumidifiers. This new input output connection is routed by a CAT-5 cable to the PWX J-1 terminal. An adapter was attached to the J-1 female terminal for easier wiring of selected ports. To be able to read and write the voltage and current from the PWX, pins 21–25 need to be accessed via the CAT-5; the wiring has been configured to allow the PWX, which cannot sit in the shed for long period of time due to lack of environmental protection features, to be removed easily when necessary. Figure 10 shows the rear facing view of the PWX with J1 in the lower left and configuration specifications and notes for use of the PWX may be found in Appendix C.

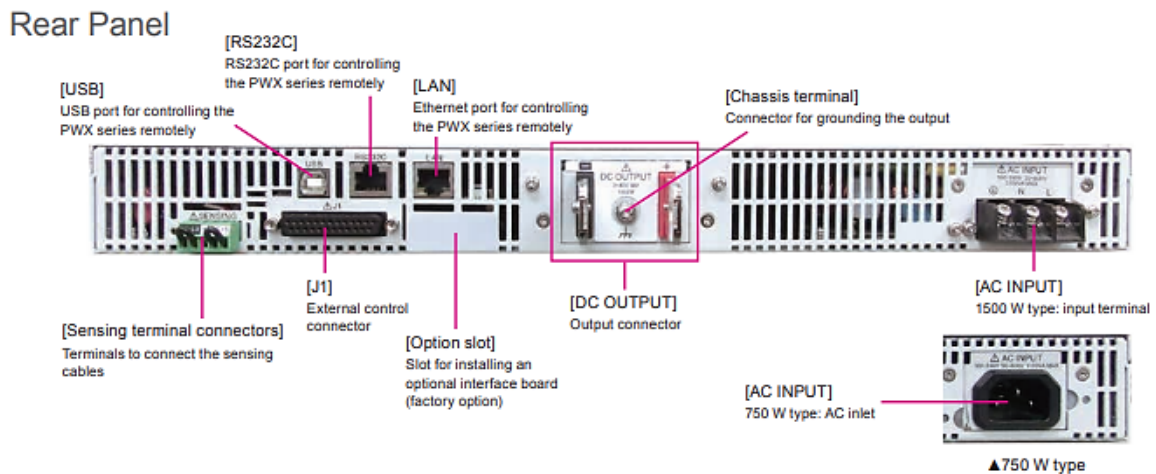


Figure 19. PWX1500ML Rear View [25]

For future control of the system, the LAN or USB terminals may be used in conjunction with the control system however the LAN was already being used for active data sharing and control with the graphics display to be investigated later and the USB terminal required advanced software that does not couple with the Allen Bradley software. If component downsizing were required (removal of steady relays) this power supply and

overall microgrid feature enough “smart” systems that if could achieve rudimentary autonomous function with the need for base logical control.

The other significant challenge of running components off the microgrid is meeting each of the component’s specific energy needs. The utilization of the inverter and power supply is the simply but bulky way of meeting this need while allowing for easy adaptability and sizing. Table 1 shows the specific voltage type and current for each generation subsystem component. The controller itself powers other critical components like the PID valve for oxygen release as well as providing the current required to measure the water levels of each of the tanks. This means that the current draw for the controller itself is assumed negligible but may increase depending on the extended modules and what is running at any given time. The biggest concern in meeting the components voltage needs is keeping in phase and not pushing over voltage. With this in mind, the PWX and inverter each feature overvoltage protection as well as undervoltage internal protection to keep systems, especially the unique electrolyzer, from breaking.

Table 1. Generation Power Draw Specifications

Component	Voltage Required	Estimated Current Draw
Electrolyzer	12-13 VDC	14.7 A
Dehumidifiers (4)	11-14 VDC	2.7 A each
Micro850 Controller	120 VAC	< 5 A
Control Valves	120 VAC	< 1 A

The negatives of the “bulky” PWX-Inverter coupling mainly come from excess power draw and losses from conversion but these modern technologies have relatively low steady draws given their capabilities. The rated draw for the PWX without the bleeder circuit running is .1 mA while the inverter’s power on rating is 1.2 A provided. The inverter feed current is not considered a loss because this feeds the constantly running controller that regulates the whole system. Also the inverter features an undercurrent and undervoltage switch which automatically meets load demand with plug in power when

required. This feature is in place for safety and simplicity at the moment but the plug in may be removed at any time for full microgrid utilization. Table 2 shows the maximum voltages for each component as well as the overall capacity; again, the “bulky” microgrid components are meant for upscaling without a major penalty for power conversion or constant autonomous operation. Peak efficiency is not the goal of this rig and the supply from the solar panels coupled with the battery capacity should lead to seamless running of all systems components.

Table 2. Generation Microgrid Component Specifications

Component	MAX Input : Output	Capacity
Solar Panels (9)	~ : 86 VDC(full sunlight)	6200 W
Charge Controller	240 VDC : 12/24/48 VDC	6600 W
Battery Bank (2)	12 VDC 200 ah	~
Inverter	16 VDC : 120 VAC	4000 W (6000 W peak)
PWX1500 Power Supply	120 VAC : 84 VDC	1500 W

C. CONTROLLER LOGIC AND OPTIMIZATION

The existing connections between the generation rig and the controller have already been discussed in the component overview however the logic behind the connections and relays has not. The logic before microgrid implementation had two main sections: water production/channeling and oxygen exhaust. If the water levels for the storage tanks were below the maximum, the dehumidifiers would run continuously due to a constant supplied voltage. If the water levels in either process tank lowered below the minimum, they would be resupplied by the storage tanks via gravity feed. For the oxygen exhaust, the water tank level of the oxygen process tank correlated to the pressure of the generated oxygen. In order to keep the pressure normalized within the electrolyzer, Fosson [13] wrote a PID controller code to exhaust the oxygen in order to keep the process tank water level nearly constant. All of this logic assumed a constant power supply and still relied on human operation to

ensure that overpressure does not occur if the hydrogen gas is not simply being exhausted as well.

In order to add on power consumption logic as well graphics interaction with the system, the following steps were taken in the connected components workbench (CCW) script; the script itself may be found in Appendix D for reference and future iterations. The inputs to the controller were modified slightly to best understand the status of the MEG as well as the power being transmitted to the major components. As such, the current transducer now reads the current provided to the battery bank in order to confirm that the solar panels are providing power to the system. The exact values could be recorded for data collection purposes as well as overall autonomous logic for when to operate the system at maximum capacity. The first voltage transducer still reads the voltage provided to the electrolyzer; this is a redundancy as the voltage provided by the power supply is already routed to the controller but this is the most critical system so an accurate reading of exact voltage applied is required. The second voltage transducer is attached to the battery bank to evaluate depth of discharge (DOD) and avoid overdrawing the battery to cause permanent damage and analyzing trickling. Figure 20 shows the charge characteristics of this specific lead acid gel battery after certain sustained DOD's. The scales are per cell with each battery featuring six cells. This again is a redundancy as the internal undervoltage protection of the inverter will automatically switch to macro-grid power in the case of undersupply by the battery. The switch in the inverter is programmed for under 10 volts and may be overridden if necessary. The correlation with the battery discharge parameters will be investigated further in the discussion section.

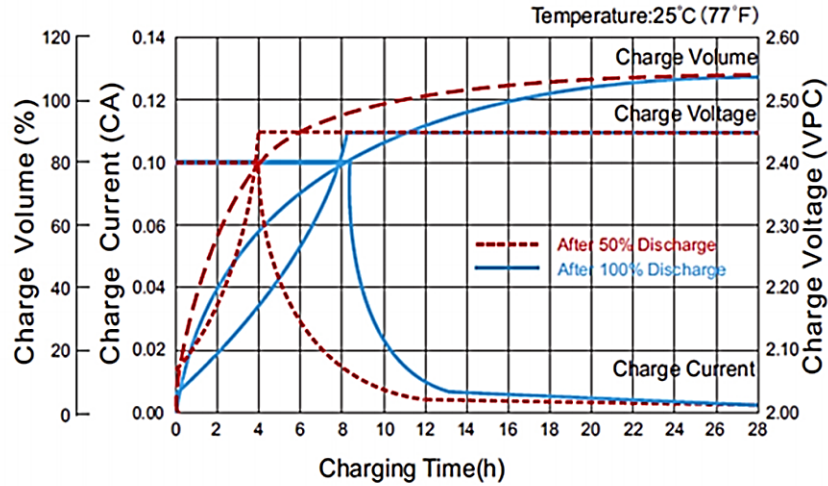


Figure 20. Lead Acid Hybrid Gel Discharge Characteristics [25]

To allow for user interaction with the graphics, new global variable inputs were applied to the code and to button modules within the applet, to be further explained in the graphics section. The first button serves as a secondary on/off switch outside of the physical emergency stop button located on the front of the rig. This visual on/off switch allows for singular startup and manual override of the autonomous system when required. The other interaction with the system relates to the output of the dc power supply to the electrolyzer. Because this is the most vulnerable system to over/under current, variability in the applied current is required for sustained autonomous operation while still ensuring the system is operating efficiently. With the entire system online including compression, the generation mass flow will exceed the flow compressed by the steady state compressor, leading to a significant buildup and decrease in compression efficiency. To combat this, the code or user input may be used to increase or decrease production rates from the electrolyzer. Currently, this user input is a simple switch turning the system from max capacity to nominal or efficient operation. If the pressure levels increase too significantly, controller logic in place looking at the hydrogen process tank water level will trigger a shutdown of the electrolyzer completely.

There was limited optimization of the controller due to the lack of flow rate or other performance metric data acquirable by the system. The Alicat flow rate meter cannot

currently transmit data to the controller to create logic that can vary the voltage and current supplied for maximum output. The storage water tank levels could also be monitored to quantify the amount of water produced by the electrolyzers for a given power drain but the losses from evaporation are nonlinear and would significantly skew this data. As has been mentioned multiple times, the goal of this rig is not optimization in terms of production or compression but rather optimization of power usage for scaling purposes and lowering the cost of COTS products.

THIS PAGE INTENTIONALLY LEFT BLANK

V. CONCLUSION AND RECOMMENDATIONS

In the continued pursuit of a fully autonomous, robust hydrogen generation and compression platform, this work provides the critical integration of a new renewable energy source to decouple from on grid power. To increase ease of use, the app was designed for simply integration with the graphics interface to monitor as well as control the system effectively from one point. While the efficiency of the microgrid power supply was not a significant criteria in selection and implementation, the batteries coupled with advanced power supply and inverter have proved to be a safe and reliable system capable of meeting hydrogen generation component needs while also power generation components. The inverter's automatic AC switch provides redundancy in protecting the batteries from overdraw as well as sustained operation if other power sources are available and solar is not providing enough alone. Previous research on solar panel efficiency by Aviles [15] provides enough insight into the power that would be provided by the panels so their lack of integration in the system did not result in a failure to prove the microgrid works properly. The actual discharge characteristics of the battery though will need to be tested once implemented in the system.

The new interface continues a simplification process initiated by Lewis [24] to allow for seamless upgrading and scaling of this rig. Any user can now monitor the status of all generation components and control how the system is running at the push of a single button while the code optimizes the utilization of energy from the battery bank. This interface coupled with oversized power supply allows for the scaling of this system if required for a real world test with higher flow rates. For example, the 2000 W rated inverter and 4000 W power supply are both capable of power draws 100x the current utilization of the generation side so the only requirements for scaling would be larger or additional electrolyzers and steady state pumps as well as a larger solar panel array. The final step for full proof of concept of this rig will be autonomous control and routing of the compressed hydrogen through the system using high pressure, digitally controlled valves. Once this is completed, this will truly be a robust hydrogen fuel manufacturer running on renewable energy and ambient moisture with zero user input required.

The steps required to achieve this ultimate proof of concept include increased controller capabilities, integration of each system back in the same space as safety regulations allow, and flow rate control and routing. The data acquisition and storage restraints of the current Micro850 controller along with the current maximum utilization of expansion modules are both justifiable reasons to seek an upgrade. Added input and output modules or simplifications of current systems would mean better communication with the system and the user. This could be coupled with the reduction in system size to a CONEX box as the controller itself doesn't necessarily need to be smaller but rather more advanced in processing and storing information. Even if the current set of read/write capabilities are acceptable, the generation and compression systems currently use two separate controllers. An upgrade to one, highly advanced controller coupled with a reduction in required inputs and outputs for logic execution would significantly add to simplicity and ease of use.

Finally, the highest priority step towards autonomous operation will be actively regulating production and routing the high-pressure hydrogen. This is currently being done manually through the DC power however having a flow rate meter from the exit of the electrolyzer and compressor would allow for exact power utilization to avoid overflow or excessive power waste. If additional flow rate is not required or desired, then proper, lower capacity components will be necessary for efficiency. Implementing this could be done through the connected components software with serial inputs from the Alicat flow meters but the restrictions on data processing of the Micro850 would make it difficult to utilize this data effectively. If another controller is pursued or even a computer system is implemented, the PWC is capable of taking set timetable inputs and executing the outputs based on the time plot. For example, if the system knows the sunrise was at 0600, it could prep the compressor to take higher flow rates and then read the flow data from the system. Then during steady state operation when the flow rate is known entering and exiting the compressor, changes can be made to the electrolyzer power supplied to slow or accelerate production.

The final step in routing the high pressure gas can only be executed after the proper compressor has been equipped with a sufficient flow rate where a single bottle may be filled. Until this happens, routing is useless because a user can manually change tanks

based on the slow flow rate. If this is achieved, the cost of an automated, high pressure routing system may outweigh the benefit depending of the DOD's desired utilization of Hydrogen from this system. If many small tanks need to be filled for drones, then routing would be necessary to ensure there are high pressure tanks available at all times without the need to bring one back for a refill. This shift in focus towards filling many smaller bottles also goes along with the goal of downsizing to a Conex box or a towable, smaller container. Once a direction is set, all funding should be directed towards this specific goal as the alternative of trying to achieve many small things on this system would render previous work and money spend obsolete for the pursuit of another goal. The original concept from 2016 remains with added control features, energy processing, and compression but the idea of running forward operating bases off of stand along hydrogen gas stations holds the same challenge it did before. This system is close to achieving the proof of concept that started back then but the exact need of the DOD must be identified in order to properly move forward and finish the job.

THIS PAGE INTENTIONALLY LEFT BLANK

APPENDIX A. INVERTER SPECIFICATIONS



Figure 21. Inverter Front View

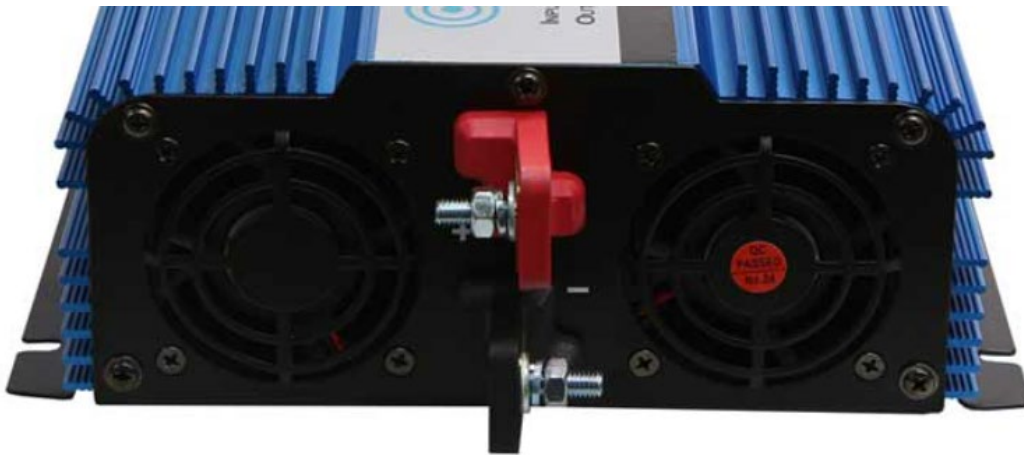


Figure 22. Inverter Rear View

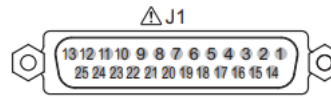
The following is basic information about the 2000 W pure sine power inverter to serve as a basic user's manual. The inverter requires manual input to power on once hooked up to DC power and will require DC power to illuminate the indicator light and enable the alarm features. If hooked up to AC power, the bypass will function properly even if the inverter is not hooked up to a DC supply (the power indicator light will be off).

- 2000 watts continuous
- 4000 watt surge (not recommended for start up applications)
- Built in transfer switch 25 amp transfer <20 msec
- Bypass/throughput = 25 amps do not exceed. Damage to the inverter will occur and void warranty
- DC input voltage 10–16V
- AC input voltage 120VAC +/-10%
- Output voltage 120VAC, 60HZ
- Efficiency 86–90%
- THD: <3%
- Over voltage shutdown 16VDC +/- .5V
- Under voltage shutdown 10VDC +/- .5V
- Under voltage alarm 10.3VDC +/- .3V
- Over temp protection 150 degrees F +/- 5 degrees F
- Thermal fan
- Pure sine output
- No load current: 1.2A (power switch on)
- Direct connect terminal block
- L x W x H: 21.5" x 9.5" x 3.5"

APPENDIX B. PWX1500 SPECIFICATIONS AND TIPS

The following is an overview of the control and system functionality of the Kikisui PWX1500 DC power supply. This highly advanced power supply has communication interfaces through the J1 control point as well as USB and ethernet connections. The use of these connections is however not trivial. The configuration settings can be found in the user manual referenced. The configuration section is over 6 pages and highlights each specific function modification, most of which are not relevant to this work. The configuration must be set for the desired communication protocol as well as the required system functionality on startup and nominal operation. See the notes section for assistance with initial setup and troubleshooting.

J1 connector pin arrangement



Pin number positions when you are facing the rear panel

Connector type	5747461-3 (AMP)
Plug type	745211-7 (AMP)
Wire diameter	AWG26 to AWG22
Manual pressure welding tool	AMP handle assembly 58074-1 AMP head assembly 58063-2
Insertion/extraction tool	AMP 91232-1 or equivalent

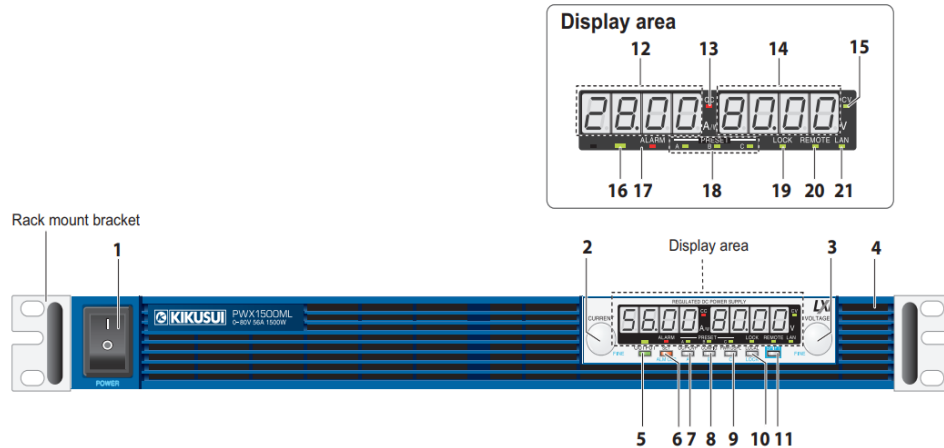
Pin no.	Signal name	Description
1	STATUS COM	Status signal common for pins 2, 3, and 14 to 16. ¹
2	CV STATUS	On when the PWX series is in CV mode (open-collector output from a photocoupler). ²
3	CC STATUS	On when the PWX series is in CC mode (open-collector output from a photocoupler). ²
4	N.C.	Not connected.
5	ALM CLR	Alarm clear terminal. Alarms are cleared when a LOW (0 V to 0.5 V) or short-circuit is applied to this terminal.
6	SHUT DOWN	Output shutdown control terminal. The output is turned off when a LOW (0 V to 0.5 V) or short-circuit is applied to this terminal.
7	PRL IN-	Negative input terminal for master-slave parallel operation.
8	PRL IN+	Positive input terminal for master-slave parallel operation.
9	PRL COMP IN	Correction signal input terminal for master-slave parallel operation.
10	A COM	External signal common for pins 5 to 9, 11 to 13, 18, 20 to 22, 24, and 25. During remote sensing, this is the negative electrode (-S) of sensing input. When remote sensing is not being performed, this is connected to the negative output.
11	PRL OUT+	Positive electrode output terminal for master-slave parallel operation.
12	PRL COMP OUT	Correction signal output terminal for master-slave parallel operation.
13	I SUM	Current signal terminal for master-slave parallel operation.
14	ALM STATUS	On when a protection function (OVP, OVP2, OCP, OHP, OHP2, FAN, SEN, or AC_FAIL) has been activated or when an output shutdown signal is being applied (output through an open-collector photocoupler). ²
15	PWR ON STATUS	Outputs a low level signal when power is turned on (output through an open-collector photocoupler). ²
16	OUT ON STATUS	On when output is on (output through an open-collector photocoupler). ²
17	N.C.	Not connected.
18	OUT ON/OFF CONT	Output on/off terminal. On when set to LOW (0 V to 0.5 V) or shorted; off when set to HIGH (4.5 V or 5 V) or open (CF10: Lo) On when set to HIGH (4.5 V to 5 V) or open; off when set to LOW (0 V or 0.5 V) or shorted (CF10: Hi)
19	A COM	External signal common for pins 5 to 9, 11 to 13, 18, 20 to 22, 24, and 25. During remote sensing, this is the negative electrode (-S) of sensing input. When remote sensing is not being performed, this is connected to the negative output.
20	REF OUT	External resistance control terminal; 5.25 V (CF07: Lo) or 10.5 V (CF07: Hi). The maximum output current 2.5 mA.
21	I PGM ³	Terminal used to control the output current with an external voltage or external resistance. 0 V to 5 V; 0 % to 100 % of the rated output current (CF07: Lo). 0 V to 10 V; 0 % to 100 % of the rated output current (CF07: Hi).
22	V PGM ³	Terminal used to control the output voltage with an external voltage or external resistance. 0 V to 5 V; 0 % to 100 % of the rated output voltage (CF07: Lo). 0 V to 10 V; 0 % to 100 % of the rated output voltage (CF07: Hi).
23	A COM	External signal common for pins 5 to 9, 11 to 13, 18, 20 to 22, 24, and 25. During remote sensing, this is the negative electrode (-S) of sensing input. When remote sensing is not being performed, this is connected to the negative output.
24	I MON	Output current monitor. 0 % to 100 % of the rated output current is generated as a voltage between 0 V and 5 V (CF08: Lo) or a voltage between 0 V and 10 V (CF08: Hi).
25	V MON	Output voltage monitor. 0 % to 100 % of the rated output voltage is generated as a voltage between 0 V and 5 V (CF08: Lo) or a voltage between 0 V and 10 V (CF08: Hi).

1 The status common is floating (isolation voltage of 60 V or less), it is isolated from the control circuit. If connected for master-slave parallel operation, STATUS COM of the master unit will be connected to A COM of the slave unit (it will no longer be floating).

2 Open collector output: Maximum voltage of 30 V and maximum current of 8 mA.

3 When using the isolated analog interface (Option), do not apply signals to VPGM (pin 22) and IPGM (pin 21).

Figure 23. PWX1500 Pin diagram overview. Source: [28].



No.	Name	Function	See
1	POWER switch	Flip the switch to the (I) side to turn the power on. Flip it to the (O) side to turn the power off.	p. 15
2	CURRENT knob	Used to set the current value or select a parameter number in the CONFIG settings.	p. 33, p. 48
	FINE	Used to make fine current value adjustments.	p. 33
3	VOLTAGE knob	Used to set the voltage value or change the value of a CONFIG parameter.	p. 33, p. 48
	FINE	Used to make fine voltage value adjustments.	p. 33
4	Air inlet (louver)	Air inlet for cooling the inside of the PWX series.	–
5	OUTPUT key	Used to turn output on and off.	p. 35
6	SET key	Used to set and confirm the output voltage and output current (the key has an LED).	p. 32
	ALM CLR key	Used to release protection functions that have been activated (the key has an LED).	p. 42
7	OCP • OVP keys	Used to set and display the overcurrent protection (OCP), overvoltage protection (OVP), undervoltage limit (UVL) trip points (the key has an LED).	p. 43
	A	Used to recall and save the value of preset memory A (the key has an LED).	p. 61
	CONFIG key	Used to configure the various operating conditions (the key has an LED).	p. 48
	B	Used to recall and save the value of preset memory B (the key has an LED).	p. 61
	PWR DSPL key	Used to display the output power on the ammeter (the key has an LED).	p. 32
	C	Used to recall and save the value of preset memory C (the key has an LED).	p. 61
	LOCAL key	Used to switch between local mode and remote mode (the key has an LED).	p. 65
10	LOCK key	Used to lock the operation of all keys other than the OUTPUT key (the key has an LED).	p. 63
11	SHIFT key	Used to enable the functions that are written in blue characters below the key.	–
12	Ammeter	Displays the current, power, or the parameter number of a CONFIG parameter.	p. 32, p. 48
13	CC LED	Lights in red during constant current mode.	p. 40
14	Voltmeter	Displays the voltage, the value of a CONFIG parameter, or the cause of an alarm.	p. 32, p. 41, p. 48
15	CV LED	Lights in green during constant voltage mode.	p. 40
16	OUTPUT LED	Lights in green when output is turned on. Blinks orange when output is on and a protection function has been activated.	p. 35, p. 41

No.	Name	Function	See
17	ALARM LED	Lights in red when a protection function has been activated. However, does not light when a undervoltage limit (UVL) protection has been activated, Blinks red when the power limit (POWER LIMIT) has been activated.	p. 41
18	PRESET LED	A: Lights in green when the memory A values are being recalled or saved. B: Lights in green when the memory B values are being recalled or saved. C: Lights in green when the memory C values are being recalled or saved.	p. 61
19	LOCK LED	Lights in green when the keys are locked.	p. 63
20	REMOTE LED	Lights in green during remote control.	–
21	LAN LED	Lights and blinks when the LAN interface is in use. • No fault status: Lights in green. • Fault status: Lights in red. • Standby status: Lights in orange. • WEB identify status: Blinks green.	–

Figure 24. PWX1500 front view and display. Source: [28].

Table 3. Required configuration for specific external control functionality

External Voltage Control	CF06 set to ON, CF07 set to Hi
External Current Control	CF05 set to ON, CF07 set to Hi
Voltage Monitoring	CF08 set to Hi (0-10V), Lo (0-5V)
Output on Startup	CF02 set to Safe (Output Off), Auto (set for Autonomous), Force (Output On)

Notes:

- Never leave the PWX out in the shed for multiple nights. The ambient moisture accumulates on the device which then leads to corrosion and has faulted a PWX in the past (they are very expensive and useful to the shed).
- PWX software is useful when implemented however the software interface itself is outdated and requires careful tuning. The ethernet port or USB port may be used; continuous input is required in remote operation mode. The software cannot be coupled with the controller due to lack of software integration. The Ki-VISA library is required to run the software so both packages must be downloaded at the website. There is a free trial of the software available for download with a one month (30 day) activation window.
- When mounting the PWX in the shed, face both bolts outside and ensure that the terminals are not bent or scratched significantly when installing power cables.

APPENDIX C. PANELVIEW 800 VARIATION STEPS



Figure 25. PanelView 800 Graphics Terminal rear view. Source: [27].

The following is the process for connected a PanelView 800 graphics terminal to a Micro850 for read/write control

1. Connect the PanelView 800 to the Controller using ethernet or serial connection. USB cannot be used for active data monitoring and transfer.
2. Connect your computer to the controller and start a new project. Select discover device and select the controller to add to the project. Then select the PanelView 800 within the controller section under ethernet connections if available. If not, manually select the PanelView 800 Model to be equipped.
3. Under this new project, ensure that the Micro850 ethernet port is enabled and select 'Configure IP address and settings'. For the IP address and Subnet mask, configure a new network address similar to that of the computer or one that you can remember easily. To find your computer's IP and subnet, press 'Windows Key' + 'r' and type 'cmd'. Then in the command window, type 'ipconfig/all'. There you will find your computer's ethernet address and subnet mask. The address of the computer isn't too significant (controller must have different first

two numbers) but the subnet mask must match the computer subnet mask exactly or else it will not be discoverable by the computer.

4. Once the controller ethernet IP and subnet are configured, go to communication settings on the PanelView 800. Select set static IP and you will see entries for IP and subnet just like the controller. The static IP must feature the same first three numbers as the controller with a different last number within about 20. The subnet mask must be exactly the same.
5. Finally to complete the connection, double click on the PanelView 800 icon in the device menu. Select portrait or landscape orientation and then you should see communication and controller settings. Select 'Ethernet | Allen-Bradley CIP' protocol and then select the controller type 'Micro800'. Type in the exact same IP address from the Micro850.

The following is the process for generating a tag to confirm connection:

1. Tags are the graphic's indication of input variables as well as output writable variables. To generate a tag, double click on the tag icon under the graphics terminal in the device menu.
2. In the tag editor window, generate and name a new tag and then select the address by clicking the ellipses. It will open a window with all global variables, local variables, and base input/outputs of the controller. The terminal cannot take local variables so choose or make a global variable that you want to display in some way or vary.
3. Apply this tag to a button or numerical display on the status screen. There are great videos online from Allen Bradley showing how to develop apps and screens.
4. After developing your tag, ensure there is some sort of script or ladder diagram to cause the tag to be active. Follow the next set of instructions to upload the app onto the graphics terminal.

The following is the process for downloading the app to the graphics terminal internal storage:

1. With the graphics terminal main page open, ensure that the app is validated (top left above version number). If not, click validate and ensure there are no errors or warnings. Save the project.
2. Insert an SD card or USB drive into the computer. Within the project folder, select 'PVC Project' folder and locate the .asv file. Copy the .asv file with the name of your graphics file to the SD or USB.
3. Remove the SD or USB from your computer and put into the graphics terminal. The USB port is on the rear and the SD port is on the right side.
4. In the file manager, select SD or USB as the source and the .asv file should appear. Select internal for the second entry and press copy in the top right. Step back to internal for the source and you should see the file. Press run to execute and it will load and display the app screen. If connections fail, error bars will appear for each tag that is not connected. Troubleshoot the IP addresses and gateway address.

THIS PAGE INTENTIONALLY LEFT BLANK

APPENDIX D. CONNECTED COMPONENTS CODE

Table 4. Connected Components Variable Overview

Name	Alias	Data Type	Dimension	Initial Value	Project Value	Comment	Direction	String Size
InputVoltage		SCALER			Var	
VOLTAGE		REAL					Var	
LEVEL_2		SCALER			Var	
TANK_2		REAL					Var	
VOLTAGE_MIN		REAL		10.5			Var	
LEVEL_1		SCALER			Var	
TANK_1		REAL					Var	
LEVEL_3		SCALER			Var	
TANK_3		REAL					Var	
LEVEL_4		SCALER			Var	
TANK_4		REAL					Var	
VOLTAGE_OFFSET		REAL		2.8			Var	
WATER_TOTAL		REAL					Var	
WATER_MIN		REAL		2.0			Var	
WATER_MAX		REAL		11.0			Var	
WATER_SET		REAL		9.0			Var	
INPUT_VOLTAGE_2		SCALER			Var	
ELECTRO_VOLTAGE		REAL					Var	
enable		INT					Var	
ELECTRO_VOLTAGE_OFFSET		REAL		4.5			Var	
ELECTRO_VOLTAGE_MAX		REAL		14.0			Var	
PROCESS_TANK_MIN		REAL		1.5			Var	
PROCESS_TANK_DIFF		REAL					Var	
PROCESS_TANK_SETPOINT		REAL		0.0			Var	
LEVEL		REAL					Var	
Input_current		SCALER			Var	
Current		REAL					Var	
Current_Offset		REAL		2.4			Var	
dcVoltage		SCALER			Var	
dcCurrent		SCALER			Var	
setCurrent		SCALER			Var	

The following is the exact controller code to execute the controller logic as discussed throughout the thesis. There are comments for all subsections of the code but the main logic relies on nested if statements based on controller processing capabilities.

Programs

```
(* This is the control program for the hydrogen generation side. The
purpose of this program is to capture ambient moisture and
using the hydrotube produce hydrogen and oxygen gas.*)
(*First step is to establish the emergency stop button. The
emergency stop button is normally closed. Power is routed from
the controllers 24v power supply through the emergency stop button
and back to the Input pin _IO_EM_DI_01. The embedded input board can
only
tell if a signal is present or not, it can not determine amplitude.
Any_TO_INT converts the incoming signal into either a one (1) or a
zero (0).
One (1) means that a signal is present and the emergency stop button
is not engaged. Zero (0) means that there is no signal present and
the
emergency stop button is engaged. The ENABLE parameter is used later
in the program as a requirement to turn on dehumidifiers and
hydrotude.*)
enable:= ANY_TO_INT(_IO_EM_DI_01);
(*Next step is determine voltage being supplied by the DC power
supply and voltage applied to the hydrotube.*)
(*InputVoltage is determining the amount of voltage being supplied
by the DC power supply. This is accomplished by using the DC
transducer #2.*)
InputVoltage(ANY_TO_REAL(_IO_P2_AI_00),InputVoltage.InputMin,InputVo
ltage.InputMax,InputVoltage.OutputMin,InputVoltage.OutputMax);
Voltage:=InputVoltage.Output - VOLTAGE_OFFSET;
Voltage_g := VOLTAGE;
IF Voltage_g >= VOLTAGE_MIN THEN
    batteryTag_g := TRUE;
ELSE
    batteryTag_g := FALSE;
END_IF;
(*INPUT_VOLTAGE_2 is determining the voltage being supplied to the
hydrotube. This is accomplished by using the DC transducer #1.*)
INPUT_VOLTAGE_2(ANY_TO_REAL(_IO_P2_AI_01),INPUT_VOLTAGE_2.InputMin,I
NPUT_VOLTAGE_2.InputMax,INPUT_VOLTAGE_2.OutputMin,INPUT_VOLTAGE_2.Ou
tputMax);
ELECTRO_VOLTAGE:=INPUT_VOLTAGE_2.Output - ELECTRO_VOLTAGE_OFFSET;
Electro_voltage_g := ELECTRO_VOLTAGE;
(*Determine Power consumption*)

(*This is the Current input to the Battery bank from the charge
controller*)
Input_current(ANY_TO_REAL(_IO_X3_AI_00),Input_current.InputMin,Input
_current.Inputmax,Input_current.OutputMin,Input_current.OutputMax);
Current:=(Input_current.Output)-Current_Offset;
current_g := Current;
(* This is the Voltage Output (fixed) provided by the DC power
supply*)
dcVoltage(Any_to_real(_IO_P2_AI_02),dcVoltage.InputMin,dcVoltage.Inp
utmax,dcVoltage.OutputMin,dcVoltage.OutputMax);
dcVoltage_g := dcVoltage.Output;
```

```

(*This is the Current output provided by the DC power supply*)
dcCurrent(Any_to_real(_IO_P2_AI_03),dcCurrent.InputMin,dcCurrent.Inp
utmax,dcCurrent.OutputMin,dcCurrent.OutputMax);
dcCurrent_g := dcCurrent.Output;
(* Next step is to determine the water level in the various tanks.
Tank 1 and 2 are water from the dehumidifiers. Tank 3 and 4 are the
process tanks
connected to the hydrotube. Tank 3 is the hydrogen process tank, and
Tank 4 is the oxygen process tank. The output is inches of water*)
LEVEL_1(ANY_TO_REAL(_IO_P1_AI_01),LEVEL_1.InputMin,LEVEL_1.InputMax,
LEVEL_1.OutputMin,LEVEL_1.OutputMax);
TANK_1:=LEVEL_1.Output;
TANK_1_g := TANK_1;
LEVEL_2(ANY_TO_REAL(_IO_P1_AI_01), LEVEL_2.InputMin,
LEVEL_2.InputMax, LEVEL_2.OutputMin, LEVEL_2.OutputMax);
TANK_2:=LEVEL_2.Output;
TANK_2_g := TANK_2;
LEVEL_3(ANY_TO_REAL(_IO_P1_AI_00),LEVEL_3.InputMin,LEVEL_3.InputMax,
LEVEL_3.OutputMin,LEVEL_3.OutputMax);
TANK_3:=LEVEL_3.Output;
TANK_3_g := TANK_3;
LEVEL_4(ANY_TO_REAL(_IO_P1_AI_03),LEVEL_4.InputMin,LEVEL_4.InputMax,
LEVEL_4.OutputMin,LEVEL_4.OutputMax);
TANK_4:=LEVEL_4.Output;
TANK_4_g := TANK_4;
(*The total amount of water available to fill the process tanks are
WATER_TOTAL.*)
WATER_TOTAL:= TANK_1 + TANK_2;
(*PROCESS_TANK_DIFF is the difference in tank level between process
tank 3 and process tank 4.*)
PROCESS_TANK_DIFF:= ABS(TANK_3 - TANK_4);
(*Now that the system inputs have been determined, the following is
the control logic.*)
(*First set of control logic is for the dehumidifiersbigButton. Due
to the relatively slow rate of water production
from the dehumidifiers, if the water tanks are not full the
dehumidifiers need to run a maximum output.
Max output is for all four dehumidifiers to be on and collecting
water.*)
IF bigButton = TRUE THEN
IF VOLTAGE > VOLTAGE_MIN THEN
    IF enable = ANY_TO_INT(1) THEN
        IF WATER_TOTAL < WATER_MAX THEN
            _IO_EM_DO_04:=TRUE;
            _IO_EM_DO_05:=TRUE;
            _IO_EM_DO_06:=TRUE;
            _IO_EM_DO_07:=TRUE;
        ELSE
            _IO_EM_DO_04:=FALSE;
            _IO_EM_DO_05:=FALSE;
            _IO_EM_DO_06:=FALSE;
            _IO_EM_DO_07:=FALSE;
        END_IF;
    END_IF;

```



```

ELSE
    _IO_EM_DO_04:=FALSE;
    _IO_EM_DO_05:=FALSE;
    _IO_EM_DO_06:=FALSE;
    _IO_EM_DO_07:=FALSE;
END_IF;
ELSE
    _IO_EM_DO_04:=FALSE;
    _IO_EM_DO_05:=FALSE;
    _IO_EM_DO_06:=FALSE;
    _IO_EM_DO_07:=FALSE;
END_IF;

```

(* Next set of control logic is for the hydrotube. Hydrotube has a maximum allowed voltage, which is 14 volts. Voltage greater than 14 volts can damage the hydrotube. Also the hydrotube has to have water in both process tank in order to function. Hydrotube will produce hydrogen gas at a faster rate than the compressor can process, so an increase in pressure due to build up of hydrogen gas will result in decrease of water level in process tank 3. Decrease in process tank 3 will cause the hydrotube to shut off and allow the compressor to catch up, thus relieving the pressure due to hydrogen gas accumulation*)

```

IF VOLTAGE > VOLTAGE_MIN THEN
IF ELECTRO_VOLTAGE < ELECTRO_VOLTAGE_MAX AND TANK_3 >
PROCESS_TANK_MIN AND TANK_4 > PROCESS_TANK_MIN THEN
    IF enable = ANY_TO_INT(1) THEN
        _IO_EM_DO_08:=TRUE;
        _IO_EM_DO_09:=TRUE;
    ELSE
        _IO_EM_DO_08:=FALSE;
        _IO_EM_DO_09:=FALSE;
    END_IF;
ELSE
    _IO_EM_DO_08:=FALSE;
    _IO_EM_DO_09:=FALSE;
END_IF;
END_IF;

```

(*Next set of control logic is used to set the current provided by the DC power supply to the electrolyzer and dehumidifiers. The voltage is set to constant on the PWX but the current is varried through an external voltage _IO_X1_AO_03. The voltage must be between 0 and 10 relating to a current between 0 and 56.*)

```

if electroTag = TRUE THEN
    setCurrent(ANY_TO_REAL(24),setCurrent.InputMin,setCurrent.Inpu
tMax,setCurrent.OutputMin,setCurrent.OutputMax);
ELSE
    setCurrent(ANY_TO_REAL(20),setCurrent.InputMin,setCurrent.Inpu
tMax,setCurrent.OutputMin,setCurrent.OutputMax);
END_IF;
_IO_X1_AO_03 := ANY_TO_INT(setCurrent.Output);

```

```

(*Next set of control logic is for refilling the process tank with
water as the hydrotube consumes water. If the
Process tank is less than the process tank minimum and there is
sufficient water in Tank 1 and 2, then valve will open
allowing water from Tank 1 to Tank 3 and Tank 2 to Tank 4.*)
IF TANK_3 > PROCESS_TANK_MIN THEN
    _IO_EM_DO_02:=FALSE;
ELSE IF WATER_TOTAL > WATER_MIN THEN
    (*H2 PROCESS TANK*)
    _IO_EM_DO_02:=TRUE;
    ELSE
    _IO_EM_DO_02:=FALSE;
    END_IF;
END_IF;
IF TANK_4 < PROCESS_TANK_MIN THEN
    IF WATER_TOTAL > WATER_MIN THEN
        _IO_EM_DO_03:= TRUE;(*O2 PROCESS TANK*)
    ELSE
        _IO_EM_DO_03:=FALSE;
    END_IF;
ELSE
    _IO_EM_DO_03:= FALSE;
END_IF;
(* (Next set of control logics is to regulate the building of oxygen
gas in process tank 4. There is a controlled PID valve
Which opens and closes based on the water level difference between
process tank 3 and 4. Oxygen is currently vented to the
atmosphere. *)
IF PROCESS_TANK_DIFF > PROCESS_TANK_SETPOINT THEN
    (*PID used to monitor oxygen process tank. Returns value
corresponding to
how open the proportional valve needs to be to bring the water
level difference
to zero.*)
    LEVEL:=PID_controlledValve(PROCESS_TANK_DIFF);
    (*Output voltage value to proportional valve pin
_IO_P3_AO_00*)
    _IO_P3_AO_00 := ANY_TO_UINT(abs(PID_Converter(LEVEL)));

END_IF;
ELSE
    _IO_EM_DO_00 := FALSE;
    _IO_EM_DO_01 := FALSE;
    _IO_EM_DO_02 := FALSE;
    _IO_EM_DO_03 := FALSE;
    _IO_EM_DO_04 := FALSE;
    _IO_EM_DO_05 := FALSE;
    _IO_EM_DO_06 := FALSE;
    _IO_EM_DO_07 := FALSE;
    _IO_EM_DO_08 := FALSE;
    _IO_EM_DO_09 := FALSE;
END_IF;

```

THIS PAGE INTENTIONALLY LEFT BLANK

LIST OF REFERENCES

- [1] H. Greenly, “Department of Defense Energy Management: Background and Issues for Congress,” Congressional Research Service, Washington, D.C., 2019.
- [2] G. J. Lengyel, “Department of Defense Energy Strategy: Teaching an Old Dog New Tricks,” 21st Century Defense Initiative, Washington, D.C., 2007.
- [3] S. Satyapal, “Hydrogen: A Clean, Flexible Energy Carrier,” 21 February 2017. <https://www.energy.gov/eere/articles/hydrogen-clean-flexible-energy-carrier..>
- [4] Cummins Diesel, “Power to Passenger Trains: How Hydrogen can Revolutionize Railway Operations,” 11 September 2020. <https://www.cummins.com/news/2020/02/28/power-passenger-trains-how-hydrogen-can-revolutionize-railway-operations-europe>.
- [5] T. Coffey, D. Hardy, G. Besenbruch, K. Schultz, L. Brown and J. Dahlburg, “Hydrogen as a Fuel for the DOD,” *Defense Horizons*, pp. 1–11, 2003.
- [6] A. Kovac, “Hydrogen in Energy Transition: A Review,” *International Journal of Hydrogen Energy*, vol. 46, no. 16, pp. 10016-10035, 03 March 2021.
- [7] “Hydrogen Production: Natural Gas Reforming,” 23 November 2020. <https://www.energy.gov/eere/fuelcells/hydrogen-production-natural-gas-reforming>.
- [8] H. K. Chang, Y. H. Jae, L. Hankwon, Y. L. Kwan and K. R. Shin, “Methane steam reforming using a membrane reactor equipped with a Pd-based composite membrane for effective hydrogen production,” *International Journal of Hydrogen Energy*, vol. 43, no. 11, pp. 5863–5872, 15 March 2018.
- [9] Office of Renewable Energy, “Hydrogen Production,” 12 December 2018. <https://www.energy.gov/eere/fuelcells/hydrogen-production>.
- [10] O. Ulleberg, T. Nakken and A. Ete, “The wind/hydrogen demonstration system at Utsira in Norway,” *International Journal of Hydrogen Energy*, pp. 1841–1852, March 2010.
- [11] O. Khaselev, Turner and J. A. Turner, “High-Efficiency integrated multijunction photovoltaic/electrolysis systems for hydrogen production,” *International Journal of Hydrogen Energy*, vol. 26, pp. 127–132, 2001.

- [12] G. Sdanghi, G. Maranzana, A. Celzard and V. Fierro, “Towards Non-Mechanical Hybrid Hydrogen Compression for Decentralized Hydrogen Facilities,” *Energies*, p. 27, 17 June 2020.
- [13] E. Fosson, “Design and analysis of a hydrogen compression and storage station,” Masters Thesis, Naval Postgraduate School, Monterey, 2017.
- [14] A. Aviles, “Renewable production of water, hydrogen,,” Masters Thesis, Naval Postgraduate School, Monterey, 2016.
- [15] S. F. Yu, “Analysis of an improved solar-powered,” Masters Thesis, Naval Postgraduate School, Monterey, 2017.
- [16] G. Gabbar, “Renewable Energy Integration,” in *Smart energy grid engineering*, Amsterdam, Academic Press, 2017, p. 535.
- [17] K. Hawxhurst, “Microgrid control strategy utilizing thermal energy storage with renewable solar and wind power generation,” Masters Thesis Naval Postgraduate School, Monterey, 2016.
- [18] Google, “Monterey Satellite Map,” Monterey , 2020. <https://www.google.com/maps/>
- [19] KUS Inc., “ELLSU User Manual,” Hardware Documentation, Davie, 2017.
- [20] Omega, “SV-100 Data Sheet,” Hardware Documentation, Norwalk, 2018.
- [21] Hydrotube, “HT5-804 User Manual,” Hardware Documentation, 2014.
- [22] NEL, “Nel receives purchase orders for U.S. Navy PEM electrolyser stacks,” Cision, pp. 3–5, 09 November 2020. <https://nelhydrogen.com/press-release/nel-asa-receives-purchase-orders-for-u-s-navy-pem-electrolyser-stacks/>
- [23] Allen Bradley, “Micro850 Programmable Logic Controller Systems,” Hardware Documentation, 2013.
- [24] J. Lewis, “Implementation of an Industrial Control System for the Generation, Compression, and Storage of Hydrogen Gas from Renewable Sources,” Masters Thesis, Naval Postgraduate School, Monterey, 2021.
- [25] Renogy, Deep Cycle Gel Battery, Ontario, 2019. <https://www.renogy.com/deep-cycle-hybrid-gel-battery-12-volt-100ah/>

- [26] AIMS Power, “2000 Watt Pure Sine Inverter Specifications Sheet,” Hardware Documentation, Reno, 2019.
- [27] Allen Bradley, “2711R PanelView 800,” Hardware Documentation, 2015.
- [28] Kikusui, PWX User’s Manual, Hardware Documentation, Chicago, 2019.

THIS PAGE INTENTIONALLY LEFT BLANK

INITIAL DISTRIBUTION LIST

1. Defense Technical Information Center
Ft. Belvoir, Virginia
2. Dudley Knox Library
Naval Postgraduate School
Monterey, California